1-1-2006

Development of Power Flow with Distributed Generators and Reconfiguration for Restoration of Unbalanced Distribution Systems

Sarika Khushalani

DEVELOPMENT OF POWER FLOW WITH DISTRIBUTED GENERATORS AND RECONFIGURATION FOR RESTORATION OF UNBALANCED DISTRIBUTION SYSTEMS

By

Sarika Khushalani

A Dissertation
Submitted to the Faculty of
Mississippi State University
in Partial Fulfillment of the Requirements
for the Degree of Doctor of Philosophy
in Electrical Engineering
in the Department of Electrical and Computer Engineering

Mississippi State, Mississippi

September 2006

DEVELOPMENT OF POWER FLOW WITH DISTRIBUTED GENERATORS AND RECONFIGURATION FOR RESTORATION OF UNBALANCED DISTRIBUTION SYSTEMS

By

Sarika Khushalani

APPROVED:

Noel N. Schulz Associate Professor of Electrical and Computer Engineering (Major Professor and Director of Dissertation)	Eric Hansen Associate Professor of Computer Science and Engineering (Minor Professor and Committee Member)
Randolph F. Follett Assistant Professor of Electrical and Computer Engineering (Committee Member)	Herbert L. Ginn III Assistant Professor of Electrical and Computer Engineering (Committee Member)
Nicholas H. Younan Professor of Electrical and Computer Engineering (Graduate Coordinator)	Roger L. King Associate Dean of the College of Engineering

Name: Sarika Khushalani

Date of Degree: December 9, 2006

Institution: Mississippi State University

Major Field: Electrical Engineering

Major Professor: Noel N. Schulz

Title of Study: DEVELOPMENT OF POWER FLOW WITH DISTRIBUTED GENERATORS AND RECONFIGURATION FOR RESTORATION OF UNBALANCED DISTRIBUTION SYSTEMS

Pages in Study: 107

Candidate for Degree of Doctor of Philosophy

With the increasing interest in distribution automation, distribution power flow is important for applications like VAR planning, switching, state estimation and especially optimization. Typically, a distribution system originates at a substation and continues to a lower voltage for delivery to the customers. There are several tools for transmission system analysis. These tools include Newton Raphson, Gauss Seidel and fast decoupled techniques. These techniques however sometimes fail to converge when applied to distribution systems due to their higher resistance/reactance (R/X) ratio of the lines, making them ill conditioned. Distribution systems typically have a radial topological structure where the loads are not always constant power. With the increase in distributed generation (DG) there is a critical need to develop analysis tools to study the effect they will have on the distribution systems. Also, shipboard power systems are different from terrestrial distribution systems, as they are tightly coupled and have multiple generators.

This dissertation focuses on developing a software program to perform the power flow analysis of terrestrial as well as shipboard power systems. Components are modeled considering the mutual coupling of cables and the tightly coupled nature of the ship systems. The algorithm is built and tested on IEEE test cases. The distributed generator is modeled as both a PQ (constant power factor) and a PV (constant voltage) node.

This dissertation also focuses on reconfiguration for restoration of unbalanced distribution systems. Reconfiguration is changing the status (OFF/ON) of switches and reconfiguration for restoration is changing the switch status to maximize the supply to loads that are left unsupplied after fault removal. Methods exist for restoration of distribution systems and can be categorized into heuristics, knowledge based, meta-heuristics and intelligent techniques. However, the application of these methods have not considered the unbalanced nature of distribution system operation with mutual coupling. The restoration in this dissertation is achieved using optimization with multiple objectives; that of maximizing the load giving priority to vital loads and minimizing the number of switch operations. Also a restoration scheme for shipboard power systems with an IPS and distributed generation has been developed. Restoration with possible islanding is demonstrated.

DEDICATION

I would like to dedicate this research to my husband and my parents.

ACKNOWLEDGMENTS

I would like to express my deepest thanks to my advisor, Dr. Noel N. Schulz, for her support, guidance and constant encouragement. She not only made me academically sound but also enlightened my personality. She gave me opportunities to present at several conferences, which widened my view and gave me recognition.

I would also like to thank my committee members, Dr. Randolph Follett, Dr. Herb Ginn and Dr. Eric Hansen, for their support and valuable comments. Also their classes gave me necessary knowledge and software skills to fulfill my research work. Thanks are also due to Dr. Mack Grady and Jeffrey Billo at University of Texas, Austin for their initial work on restoration using optimization.

I gratefully acknowledge the financial support of the Office of Naval Research. Special thanks to all the technical staff and graduate students working on the E-ship project. I would also like to thank Dr. S.A. Khaparde and Dr. S.A. Soman from IIT, Bombay for their valuable discussions.

I wish to acknowledge the blessings of my parents, which helped me, climb the first steps of higher education. I am particularly grateful to my husband for his support in all ways and at each phase of my dissertation. The constant encouragement of my sister and brother is a key factor of my success.

TABLE OF CONTENTS

CHAPTER Page

LIST OF TABLES

TABLE Page

LIST OF FIGURES

FIGURE Page

CHAPTER I

INTRODUCTION

1.1 Introduction to Reconfiguration for Restoration

Recently, there has been a growing interest in Distribution Automation (DA). One of the DA functions is reconfiguration. Reconfiguration is the process of altering the configuration of the distribution system by changing the status of the switches without violating operating constraints. Reconfiguration is mainly done for loss reduction, relief of overloads (load balancing), volt/var support, and restoration. Reconfiguration for restoration involves restoring power to outage portions of the feeder, which improves service to loads by reducing outage time. Service restoration after a fault, usually referred to as emergency service restoration, has become important as distribution systems are becoming automated. Restoration is a combinatorial problem and must be implemented as quickly as possible. The basic objective of the restoration is to maximize the number of loads supplied and to minimize the switch operations involved in the restoration process. Switch minimization is essential to reduce the wear and tear of switches and manual operations for non-automated switches.

This research work deals with reconfiguration for restoration of Shipboard Power System (SPS) and Terrestrial Distribution Systems (TDS). The TDS are unbalanced with mutually coupled cables and have different operating criteria than the SPS. Further sections discuss these differences in detail. Before the Integrated Power Structure (IPS)

of the ship, the SPS reconfiguration consisted of a manual process. Circuit breakers would detect a fault situation and trip in order to isolate the disturbance. Many loads were left without supply, especially if they were downstream of the fault on a radial system. The IPS requires automated reconfiguration. Restoring vital loads quickly and efficiently will improve fight through and survivability capabilities. For the TDS, reconfiguration helps to restore the vital loads and maintain their continuity of operation. Knowing the steady state operating conditions of a power system is essential. Restoration may require solution of hundreds or even thousands of states of the system, which need repeated solution of power flow. In these applications, solving the power flow efficiently is essential. A power flow solution is thus necessary for planning and operating TDS and SPS.

1.2 Introduction to Unbalanced Distribution Power Flow

Determination of the steady state behavior of the system is the foremost step to be performed. In power systems, this calculation is the steady state power flow problem. Thus, a power flow study is a steady-state simulation of the power flows in power system circuits and can determine bus voltages and angles for specified system operating conditions. These operating conditions may benormal or emergency operating conditions, present or future conditions. The results of a power flow study can be used for planning, voltage profile, kW and kVAR losses, transformer tap settings, and to specify equipment and system capabilities and limitations. The power flow study is a very useful tool for system design and expansion, and for the economic planning and operation of large, complex, power systems. The power flow study is a first step in a stability study to

establish power flows and machine power angles before the initiation of a disturbance. The fields of power system optimization and distribution automation especially use this study, since they need repeated fast power flow solutions.

Cables in TDS and SPS provide service to unbalanced three-phase, two-phase and single-phase loads. This service leads to unbalanced three-phase voltages and currents, which necessitate three-phase unbalanced power flow analysis. A terrestrial system and ship distribution system may consist of

- Three-phase primary main feeder
- Three-phase, two-phase, and single-phase laterals
- Inline transformers
- Shunt Capacitor Banks
- Distribution Transformers
- Three-phase, two-phase and single-phase loads

Three different types of requirements can play a role in specifying the load; constant power, current, or voltage requirements. The power flow equations are non-linear equations, and solving the equations requires iterative methods. The introduction of small capacity generators, called Distributed Generators (DG), to the distribution systems necessitates that their modeling be included with other component models for the power flow analysis.

1.3 Introduction to Distributed Generators

DG is not a new concept in the power industry. It was previously called the backup generator. With the emergence of an era of deregulated power systems, several

generators are being installed on the consumer side. The rise of demand of power has lead to installation of these small power units, which give high fuel flexibility. DG, if properly planned and controlled, can be beneficial to the power industry as it can help defer the costs of expansion, and can have positive environmental impacts. DG can be defined in several ways [1], some of which are listed here:

1. Any qualifying facility under the Public Utility Regulatory Policies Act of 1978 (PURPA)
2. Any generation interconnected with distribution facilities.
3. Residential or commercial back-up generators.
4. Any on-site generation between 10 kW to 50 MW range.
5. Generators located at or near a load center.

Photovoltaics, microturbines, flywheels, batteries, fuel cells and reciprocating engines are DGs with different technologies. Figure 1.1 shows a distribution system with several DGs. DG can cause bidirectional flow of current, necessitating the alteration of already existing protection schemes. In a radial system, fault schemes like over-current schemes are used that now need to be changed to directional schemes. In the presence of a fault and during a reclosing sequence, a DG can feed the fault, prevent the reclose, and lose synchronism during this sequence. DG also modifies the reach (minimum fault current) of the relay, and can cause false trips.

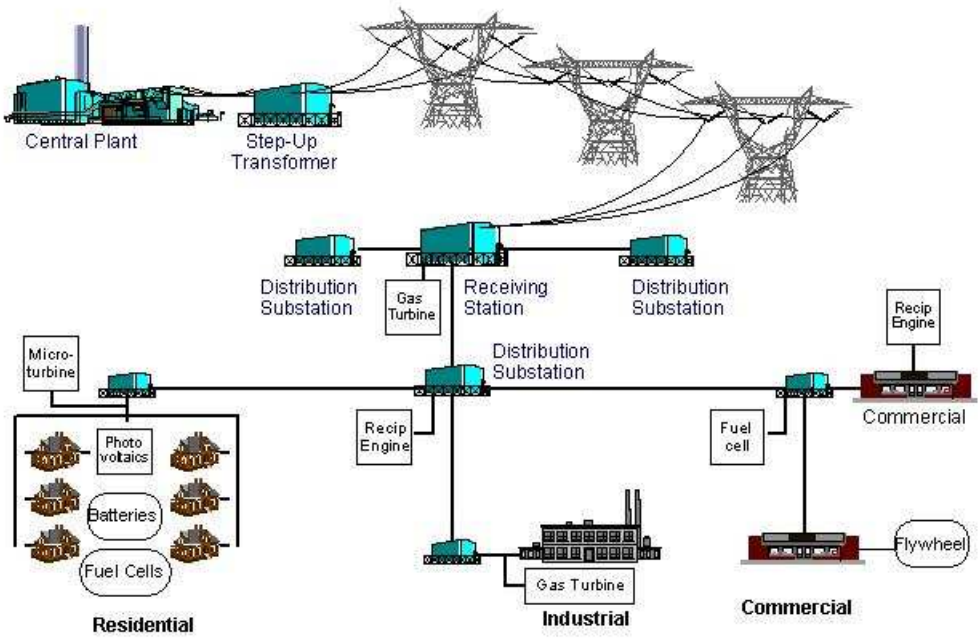

Figure 1.1: Distribution System with DG [2]

However, ways exist to overcome these inefficiencies, leading to shorter fault durations for equipment, thereby increasing reliability. The other concerns, related to power quality, include voltage deviations and sags, unbalanced phase voltages and currents, flicker and waveform distortions. The ratio Isc/IL is the ratio of the short-circuit current available at the point of common coupling (PCC), to the maximum fundamental load current. Presently, the harmonic limits for only an Isc/IL ratio of less than 20 are included in IEEE1547 [3] and the IEEE519-1992 standard [4]. These harmonics can be overcome with new converter technologies, and DG can improve voltage support.

Advantages of DG greatly depend on the site and size of DG, which also impact losses and the voltage profile. Several optimization routines can be established to find the best position of the DG for achieving a particular objective. Most utilities use the same

rules as that of capacitor placement for the DG siting. However, this subject has been dealt with in another collaborative research work [5].

When a DG or several DGs energize a portion of the utility system that has been separated from the main utility system it is called islanding. Islanding can be either intentional or unintentional. In intentional islanding, the utility intends to provide power to some consumer loads through the DG even after the utility is disconnected from the system. This type of islanding increases reliability and helps maintain the continuity of supply to the important loads. A power flow should be conducted in the island in order to assure the power balance. If the DG cannot carry the entire load of the island, then part of the load should be shed. The load to be shed should be decided in an optimum manner considering all the priorities. Intentional islanding is a very new phenomenon, and the standard IEEE1547 is in the process of revision to include this method. Some important work is ongoing in the form of standards with the allowance of DG in distribution systems:

- *IEEE Standard for Interconnecting Distributed Resources with Electric Power Systems* (IEEE Standard P1547).
- *IEEE Guide for Interfacing Dispersed Storage and Generation Facilities with Electric Utility Systems* (ANSI-IEEE Standard 1001-1988) [6].
- *IEEE Standard for Conformance Test Procedures for Equipment Interconnecting Distributed Resources with Electric Power Systems* (IEEE Standard P1547.1) this would provide some tests which are to be conducted before the interconnection [7].

- *IEEE Applications Guide for Interconnecting Distributed Resources with Electric Power Systems* (IEEE Standard P1547.2) will give technical information required to follow Standard 1547 [8].
- *IEEE Guide for Monitoring, Information Exchange, and Control of Distributed Resources with Electric Power Systems* (IEEE Standard P1547.3) will help the coordination of several DGs [8].

Overall, incorporating DG into the power system requires careful study and planning. This research work helps in such a study by developing a key tool for the steady state analysis of the system with multiple DGs.

1.4 Objectives of Dissertation

Typically, a terrestrial distribution system originates at a substation and continues to a lower voltage for delivery to the customers or loads. Unlike a transmission system, a distribution system typically has a radial topological structure. This radial structure, along with the higher resistance/reactance (R/X) ratio of the lines, makes the fast decoupled Newton method unsuitable for most distribution power flow problems. Since power flow is such a fundamental calculation, and many applications use it in planning and operation, a great deal of effort of this research work is concentrated on the development of this special power flow. The objective is to take into consideration the unbalanced, multi-source operation of TDS and SPS.

This research work is thus concentrated on

- Developing a revised distribution power flow algorithm for TDS and SPS with multiple DGs and implementing and testing this algorithm on several power systems.

- Formulated the equations and constraints for optimization of outage restoration in unbalanced TDS and in SPS with IPS considering embedded DG with islanding. This formulation will be tested using LINGO and several power systems.

1.5 Outline of Dissertation

Chapter 2 reviews the existing literature on the restoration of terrestrial balanced and unbalanced distribution systems with SPS. It also reviews the work done in the area of unbalanced distribution power flow development.

Chapter 3 presents the problem statements for the restoration and unbalanced power flow problem. It highlights the necessity of this research along with the details and presents some information regarding the software used.

Chapter 4 contains the formulation of the optimization problem for restoration of unbalanced distribution systems. It gives the solution of the problem with the verification, formulates the problem for SPS, and solves it.

Chapter 5 discusses equations and models for the algorithm to solve an unbalanced distribution power flow and highlights the characteristics of the developed software implementation.

Chapter 6 summarizes the research and details future possibilities and work that can be achieved in this area.

CHAPTER II

LITERATURE REVIEW

This chapter surveys existing methods for both unbalanced distribution power flow and reconfiguration for the restoration problem of TDS and SPS.

2.1 Reconfiguration for Restoration Problem

Restoration for balanced distribution systems has been approached using heuristics [9-11], mathematical programming [12, 13], meta-heuristics[14-16] and expert systems [17, 18]. A combination of approaches [19, 20] has also occurred. However, most of the approaches use a resistive model of loads and lines and simplify the distribution system. They also make other assumptions, which ignore the basic characteristics of distribution systems. These characteristics are their unbalanced and radial nature due to varied customer demand, mutually coupled cables and higher R/X ratios. Most of the methods require running a complete power flow after each switching to determine if the constraints are satisfied. Reference [21] focuses on service restoration for an unbalanced distribution system using a hybrid flow pattern, a heuristic strategy based on a series of switch operations and solving for power flow only once. Others [22-25] do reconfiguration for loss minimization or load balancing or both, for unbalanced distribution systems using one or several power flow solutions.

The different solution approaches existing in literature to solve the distribution system restoration problem can be broadly categorized:

1. Intelligent Systems: Neural Network (NN), Fuzzy Logic, Genetic Algorithms (GA), Expert Systems, Heuristics, Knowledge-Based.
2. Meta-Heuristics: Tabu Search (TS), Simulated Annealing (SA), Particle Swarm Optimization (PSO)
3. Mathematical Programming

GA uses a candidate of solutions represented as strings to search the state space. First, the problem is encoded into real-valued representation or binary representation. Each string is assigned a fitness value, and the most fit individuals are selected. Mutation and crossover can be performed to generate good search space regions. After convergence, the strings are decoded to the original solution variables. Luan et al. [26] present a restoration strategy in distribution networks where each gene in a chromosome is represented as a switch. The authors decide the final status of the switch by graph theory, to keep the system radial. They have applied a GA-based supply restoration and optimal load shedding algorithm on an example system that is part of a practical system in the United Kingdom. One of the restoration examples by the author shows that using a DEC Alpha 433au personal workstation takes about 3.5 min of computer time for the GA to reach the supply restoration solution. Watanabe and Nodu [27] present a two-stage GA that they have applied on a distribution system with 30 nodes and 40 edges (lines). The

first stage GA creates radial network configurations, and the second stage GA searches for the sequence of switch operations for restoration.

PSO is based on the theory of swarming, in which a collection of behaviors from each individual or agent leads to the goal. Each agent has the knowledge of its best position so far, and the best position of the group so far. It tries to achieve an improved best position from its current position, velocity and distances from its best position and the group's best position so far. PSO was developed for continuous optimizations only. Mantawy and Ghamdi [28] present a reactive power optimization to minimize the active power loss in the network, while satisfying all the power system operation constraints. They have applied the algorithm to the IEEE 6 bus system and the values found for the control variables, viz. generator bus voltages, transformer tap positions and shunt capacitor banks are listed along with the objective that is the total loss. Apart from loss reduction, PSO has been used for load forecasting, and economic dispatch. Its use for reconfiguration is limited to var support.

SA is based on the process of annealing, where a piece of metal is heated to high degrees and immediately cooled. An initial configuration and initial temperature is assumed and all possible configurations at that temperature are evaluated. Then the temperature is decreased and configurations are again generated and evaluated. A new configuration is accepted when its cost is less than the old configuration. Even if the cost is greater, it can be accepted with some probability in order to avoid a local optimum. Toune et. al [29] compared four heuristic algorithms for distribution systems restoration, one of which is Parallel Simulated Annealing (PSA). According to the authors, PSA

parallels the routines of state transition to obtain better searching points by generating multiple neighboring states, rather than a single state. Chiang and Jumeau [30] present a modified SA for loss reduction, and further reduce losses in stage 2 by load balancing. They used the approximate power flow to check constraints in the initial stages of SA, when temperature is high, and utilized full power flow when temperature is low. They tested the algorithm on a 69 bus system.

Tabu Search starts with an initial configuration; it then chooses a best-cost configuration from a new neighborhood, which may have some configurations that are declared forbidden (tabu). The mechanisms of TS are intensification and diversification. Mori and Ogita [31] present a parallel TS for distribution system restoration, which decomposes the neighborhood in to sub-neighborhoods and uses multiple tabu lengths. The authors also claim that TS is more efficient than SA and GA in terms of computational efficiency and solution accuracy. Toune et al. [29] compared four heuristic algorithms, and they found that the reactive tabu search gave the best results with the best computational times.

Knowledge-based techniques involve the representation of expert knowledge as rules and an inference engine to infer from these rules. The rules are written as IF THEN statements in languages like PROLOG where the IF is the 'premise,' which, when satisfied activates the 'conclusion' part. Lee et al. [32] use strategies such as single grouping, multi-grouping and an expert system that can come up with a restoration plan for distributed automation with minimal groups and appropriate switching sequences. Liu et al. [33] propose an expert system for the distribution system restoration in which they

have constructed a knowledge base with 180 rules. Group restoration, zone restoration and load transfer perform restoration, and the implementation is done in PROLOG. Expert system rules are system specific, and they change with the system. In the same system itself, expert system maintenance is costly with increasing number of rules.

Butler et al. [34] use a fixed charge network flow method for restoration of SPS, which is essentially a linear optimization, performed using software CPLEX. They have considered distribution system loads as constant current and cables as three-phase with no mutual couplings so that the three phases could be decomposed. After decomposition three separate independent equations are formulated for each phase, which simplifies the optimization process. Only the magnitude of current is considered for calculations and bi-directional flow of current was not allowed while restoration. However, with several fault scenarios and introduction of DGs this assumption is not valid. Also, with the IPS, the SPS have AC as well as DC components.

2.2 Unbalanced Distribution Power Flow Problem

The unbalanced and radial nature of distribution systems makes it a difficult problem to solve. Reference [35] presents a method similar to the backward forward sweep method for solving the power flow for any radial system with realistic R/X ratios. This method assumes a balanced network, neglects shunt capacitance, and models the loads as constant power. The authors in [36] develop a new method for performing the power flow. However, their method is essentially the backward forward sweep method. They show that the backward forward sweep method is better than the Newton method and a method similar to backward forward sweep (which assumes flat voltage on all

buses and decides convergence on loads) under increased loading, deteriorating power factor and higher R/X ratios. Reference [37] uses a fast decoupled power flow for unbalanced radial systems and shows that the computational complexity is least when compared with backward forward, implicit Z_{bus} Gauss and Newton Raphson. Also, the fast decoupled method does not require sparse factorization as Newton Raphson and implicit Z_{bus} Gauss do. Backward forward does not have matrices involved, so it needs no sparse factorizations. The authors attribute the speed of the fast decoupled method to the constant triangular Jacobian matrix. On the other hand, reference [38] shows that the fast decoupled method diverged in some cases. They present a method essentially similar to the backward forward sweep method and claim that the computation time is lowest as compared to Newton Raphson, fast decoupled, and implicit Z_{bus} Gauss. They note that the convergence property of their method is neither affected by number of buses nor the R/X ratio. Reference [39] presents a rigid approach for distribution system power flow analysis. The authors use the implicit Z_{bus} Gauss method and state that its convergence is slow if more than one PV node occurs in the system. The systems considered are radial with only one slack and no PV node. Thus, they find the method to have a rapid convergence rate and minimum memory usage. Authors of [40] use the method in [39], i.e., the implicit Z_{bus} Gauss method, as a performance measure for their proposed algorithm. They noted that their algorithm, based on two matrices, viz. bus-injection to branch-current matrix and the branch-current to bus-voltage matrix, took less execution time and is thus robust and computer efficient. Reference [41] establishes the power flow solution for initializing EMTP simulations. They found the calculation of a starting point

for Newton Raphson is difficult. They convert the PQ and PV constraints into unconstrained components and get a Newton Raphson solution for this linearized problem. They use this solution as the starting point for the non-linear power flow. Two new forms of decoupling lead to Phase Decoupled (PD) and Sub-Phase Decoupled methods in [42]. They note that PD is the most robust method, and SPD has better performance than [39] and the power-based Newton Raphson in [43]. There are some other works [44-46] dedicated to unbalanced power flow solutions. M.S. Srinivas [47] gives a brief review of distribution power flows. Several power flow methods, based on the backward forward technique exist. They are classified as

1. Current summation methods
2. Power Summation methods
3. Admittance summation methods

The current summation method is more convenient and faster than the power summation method, because it uses only voltage and current instead of real and reactive power.

Apart from the work on radial distribution systems, researchers have also attempted to find a power flow solution for weakly meshed networks. Achieving this solution requires converting the network to a radial network first, by breaking all the loops in the meshed network. If the voltage mismatch between the breakpoint nodes is not within tolerance, then current is injected at each breakpoint node and the power flow is run again to check the voltage mismatch. This process continues until the power flow converges and the breakpoint criterion is satisfied. References [48-49] focus on such compensation-based techniques for weakly meshed systems.

Currently, few contributions exist that study the impact DG will have on distribution systems, especially unbalanced distribution systems. The authors in [50] present a three-phase co-generator model. They model the co-generators as PQ specified devices. By specifying the real and reactive power, they guarantee a balanced current source. They point out that in the case of larger co-generators, the node must be represented as a PV node, but that their model is applicable for small capacity co-generators. It should be noted that it is simple to model DG as a negative load, i.e. a PQ node, while incorporating it in the power flow software and it does not require any special calculations leading to no change in convergence. Reference [51] uses the Newton Raphson method to solve the three-phase power flow with a remote generator, which they model as a PV node. IEEE 14-118 node transmission systems are converted to equivalent three-phase data, assuming a transposed line. The authors test the results on two other systems of 15 and 155 nodes, created to depict unbalanced three-phase systems. Though methods like Newton Raphson, fast decoupled Newton Raphson and Gauss Seidel have been applied to distribution systems, they may fail to converge as distribution systems are ill conditioned and Jacobian tends to become singular. The contribution of Cheng and Shirmohammadi [52], addressing the power flow solution by incorporating DG for TDS, is the first to address the aspect of incorporating the PV model with backward forward sweep. Reference [53] applies an object-oriented approach for distribution system modeling using the Newton Raphson approach. It analyzes the effects of DG on balanced distribution systems.

Butler et al. [54] develop a three-phase power flow algorithm for SPS. Figure 2.1 shows the SPS they tested. They handle multiple sources that form the ring by collapsing them into a single source. A comparison of distribution power flows for balanced SPS is addressed by Lewis and Baldwin [55].

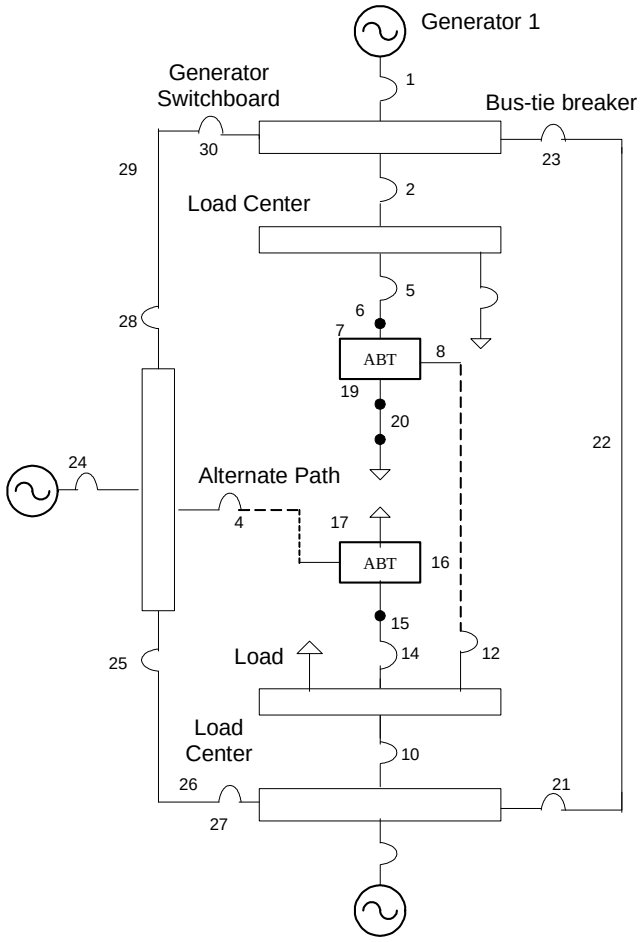

Figure 2.1: Ring Distribution System [54]

2.3 Need of this Research Work

The literature survey clearly addressed a need for an unbalanced distribution power flow solution that could give steady state solutions not only for TDS but also for SPS. This algorithm should be able to incorporate multiple DGs with no convergence

issues. The impact of DG on the existing system must be studied, because of its significant contribution in the power flow and short circuit studies. The algorithm should be able to handle large R/X ratios and should demonstrate the capability of analyzing the system for best placement and size of DG for good voltage profiles in normal conditions and after-fault conditions as well as loss reduction.

The literature survey also addressed a need for reconfiguration of unbalanced TDS with mutually coupled cables as well as SPS. A need exists for the reconfiguration of SPS with IPS. Also, with increasing interest towards small generators, having a restoration scheme considering DG and islanding becomes essential. The solution should be globally optimal with a minimum number of switching operations. This research addresses these issues and enhances the literature on power flow solutions.

CHAPTER III

RECONFIGURATION FOR RESTORATION AND UNBALANCED POWER FLOW PROBLEMS

3.1 Restoration and Reconfiguration

Distribution systems can be in normal, faulted or restored operating states. After a fault isolation, some of the un-faulted sections of the system are unsupplied. Restoration will attempt to restore most of these, or if possible, all of these loads. This chapter describes a novel formulation for a service restoration algorithm for balanced and unbalanced three-phase distribution systems. In a restored state, the inequality constraints may not be satisfied, whereas the equality constraints may be satisfied. The equality constraints are the three-phase unbalanced power flow equations; the inequality constraints are the operation restrictions imposed by the equipment. The problem of reconfiguration for restoration is a combinatorial problem where the state space to search for the solution is huge, and a complete listing of all possible states is very difficult. The problems with integer variables are NP hard (Non-deterministic Polynomial-time hard), meaning no known algorithm exists to solve these problems in polynomial time. However, the reconfiguration for restoration problem is both NP hard and NP, hence belonging to the class of NP complete problems. For these kinds of problems, the solution time increases with an increase in the number of integer variables;

however, the solution time generally depends on the formulation. Reducing the number of integer variables can also reduce the complexity of the problem, which can be achieved by formulating the problem without integer restrictions and later rounding it, but such a rounding may result in a suboptimal or non-feasible solution.

The heuristic approach of reconfiguration, which supplies the vital loads, checks the constraints, and then supplies the semi- and non-vital loads, can be used. To meet the constraints, the loads, if any, which must be shed, should be determined. This approach supplies vital loads, but it requires several power flow solutions to ensure constraints are not violated after each restoration step. These calculations are very long and take significant computation time, and they have to be performed several times. Since the speed of computation is an important factor, the heuristic technique is not a feasible approach. Thus, an optimization approach based on the classical optimal power flow problem seems better, since the power flow calculation is embedded in the optimization equations, and the equations must be solved only once rather than several times. The important aspects of this formulation are that it does not need a separate three-phase unbalanced power flow calculation, equations are not linearized, and mutually coupled cables are considered. An already-developed, three-phase, unbalanced power flow software validated the formulation.

TDS have a meshed structure with normally closed switches called sectionalizing switches and normally open switches called tie switches. The operation of these systems is radial, due to complications in protection coordination, and keeping the system radial even after restoration is thus deemed appropriate. This dissertation presents the

simulation results for modified IEEE 13-node and IEEE 37-node test cases. Since the problem size is large, it introduces switch pairs, which reduces the search space. This chapter makes a comparison of solution with and without switch pairs.

The IPS of the SPS represents better survivability in a battle situation since multiple generators can be scattered in various locations throughout the ship. Taking advantage of this survivability requires reconfiguring the power system to minimize the amount of service interruption when a portion of the system is suddenly taken out of service due to battle damage. Intelligently switching sources and shedding loads when necessary accomplishes the reconfiguration. Thus, a need exists for automated restoration schemes with minimum switching and maximum restorability. The aim is to improve the methods used to solve the reconfiguration problem for SPS. The next generation of SPS will include both centralized power sources as well as localized DG. Energy storage devices like flywheels and batteries are already on ships. Fuel cells remain another possibility. This localized DG creates a new set of constraints for shipboard system analysis relating to restoration optimization. Most distribution management systems assume a single source for distribution systems when applying various techniques and algorithms. The distribution system under normal circumstances may be expected to not operate under islanded conditions. This research work proposes restoration under islanding conditions as well.

3.2 Unbalanced Power Flow

Some of the restoration methods require the support of distribution power flow to determine the line flows and bus voltage values of the distribution system to check for

constraint violations. Thus, this research work also focuses on developing a power flow algorithm for SPS and TDS. It addresses the issues in developing the power flow algorithm. Verification occurs by comparing the results for an IEEE radial test feeder, obtained with RDAP software and developed unbalanced power flow.

A distribution system has a radial topological structure. Newton Raphson and fast decoupled Newton Raphson are the most widely used methods for transmission systems. The Newton Raphson method is computationally expensive for large systems, due to the size of the Jacobian. The fast decoupled method for transmission systems contains some approximations which allow for the decoupling of real and reactive power and voltage magnitude and angle, respectively. Since distribution systems are ill conditioned, the fast decoupled Newton method is unsuitable for most distribution power flow problems. Most of the conventional power flow methods consider power demands as specified constant values. This should not be assumed, because in distribution systems bus voltages are not controlled. Constant power, current or impedance requirements specify the loads. A three-phase method has to address issues like modeling different types of component connections, determining the starting point for the three-phase power flow solution as various shifts and transformation ratios belong to each phase and different nodes. For untransposed lines and cables, the balanced models are no longer useful. The symmetric component transform cannot decouple the three phases. Thus, the model requires a fully coupled impedance matrix in three phases. The results of power flow analysis include steady state voltages at all buses in the system, real and reactive power flows in cables, transformers and loads, power losses and reactive power generated or absorbed on

voltage-controlled buses. The power flow equations are non-linear equations, and solving those equations requires iterative methods. The backward forward sweep method is selected for the new power flow, as it involves limited matrix operations and no matrix inversions. This method iterates on a radial structure.

The SPS differs from a conventional terrestrial system as it is ungrounded and tightly coupled with much shorter cable lengths. The objective is to take into consideration the unbalanced and multi-sourced operation of SPS and TDS with DG. With the increase in number of DGs the distribution system is no longer a single source system. There has to be a change in strategy for distribution analysis. This change would require a fast power flow solution with DG. This work develops a three-phase unbalanced power flow algorithm with the choice of modeling DG as PQ or PV node. The software can handle multiple DGs and is capable of switching the DG mode of operation from constant voltage to constant power factor. This capability gives flexibility in modeling various types of DGs. The distribution system model includes modeling of lines, cables, transformers, switches, capacitors, loads and DGs. IEEE test cases are designed by the IEEE PES Distribution subcommittee for testing the three-phase unbalanced algorithm for single source systems. A DG was introduced in the IEEE 13-node test case, and the results demonstrate the effect the DG has on the voltage profile and currents. An analysis of Healy icebreaker ship was performed using the developed software. Figure 3.1 shows the United States Coast Guard Cutter (USCGC) Healy ship; Figure 3.2 shows the power system of the ship. System studies for the IEEE 37-node feeder without the regulator

show the effect of different models and varying DG penetration related to the increase in loading. System losses and voltage deviations provide the basis for comparisons.

Figure 3.1: USCGC Healy Ship [56]

3.3 Shipboard Power Systems

Reconfiguration is the key for adjusting Shipboard Power Systems (SPS) after faults. Restoring vital loads quickly and efficiently will improve fight-through and survivability capabilities. This research proposes an approach to optimize reconfiguration of SPS with IPS, which is essentially an AC-DC zonal architecture, and embedded distributed generation (DG). Currently researchers are contrasting the SPS radial distribution architecture with a zonal approach. The zonal approach employs a starboard

bus and a port bus and partitions the ship into a number of electrical zones; it is called the IPS.

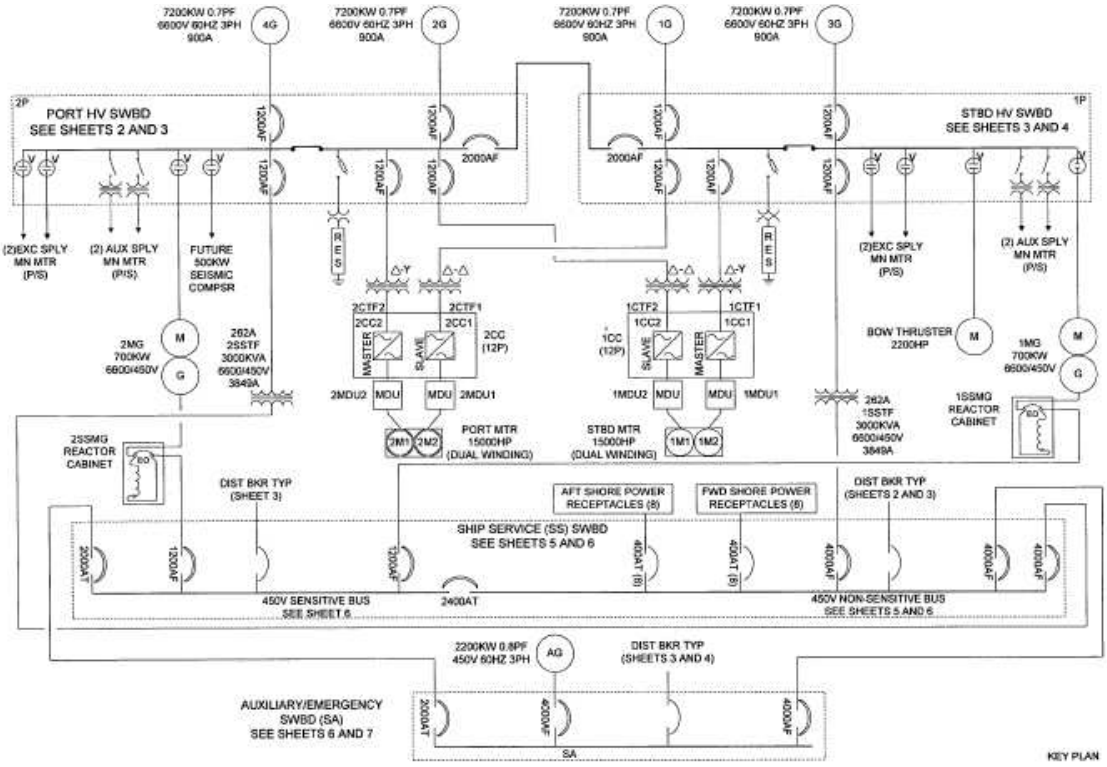

Figure 3.2: Power System of USCGC Healy [56]

The zonal architecture eliminates switchboard feeder cables running through the length of the ship, except the port and starboard cableways. In the AC distribution system, the distributed three-phase AC must be rectified, converted to 400 Hz with an inverter, shifted to an appropriate voltage level with a transformer, and then once again rectified to provide the required DC power. In the DC Zonal Electric Distribution System (ZEDS), no need exists to have an intermediate 60 Hz step. The power converts to DC at the output of the generator, and is reconverted to the form required at the point of use, so

fewer distribution transformers and AC switchgears are required and thus there is a benefit in reducing the weight and size of the ship.

The ZEDS, as shown in Figure 3.3 is one of the zonal architectures under consideration for the ship. Figure 3.3 indicates the interconnectivity and location of generators, switchboards, bus tiebreakers and zonal infrastructure. The generators supply power to the switchboard; it goes from the switchboard to the load center and from the load center to the equipment. Thus, the power is radially distributed from the generator switchboards to load. The ship is then subdivided into electrical zones. Each zone incorporates two load centers; one is fed from the port bus and the other from starboard bus. The loads are classified as non-vital, semi-vital and vital loads. Vital and semi-vital loads are those loads required for combat systems, fire systems, etc. Non-vital loads can be shed for survivability. Non-vital loads are provided from the nearest load center to minimize cable lengths. Both load centers provide power through Automatic Bus Transfers (ABT) for vital and semi-vital loads in the zone.

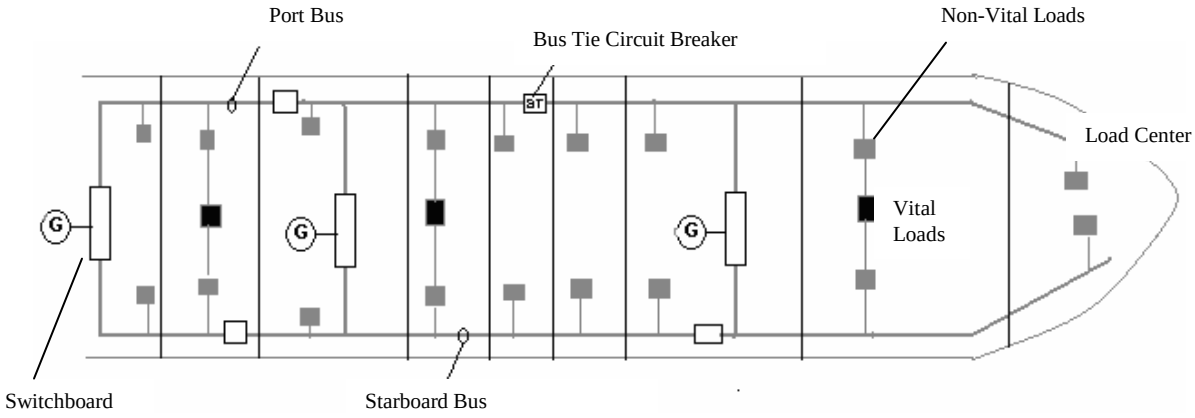

Figure 3.3: Shipboard Power System [57]

Bus ties provide longitudinal isolation between electrical zones. The next generation of SPS will include both traditional centralized power sources as well as localized distributed generation. This creates a new set of constraints in the restoration optimization. The penetration of DG within the distribution system provides a new opportunity in the area of reconfiguration in both day-to-day situations and after fault conditions.

3.4 Introduction to Software Packages

Primarily, this research used three kinds of software, viz. MATLAB, LINGO and RDAP. This section briefly introduces MATLAB, RDAP and LINGO.

3.4.1 MATLAB

MATLAB is well-known software used at universities and in research. MATLAB uses a high level language for technical computing. It has several toolboxes that are collections of functions. Its flexibility especially with matrix and vector operations provides a quick platform to program and test an algorithm. Files written in MATLAB are called m-files. For this research work MATLAB m-files were developed and built-in functions were also utilized.

3.4.2 LINGO

The LINGO commercial optimization software package from LINDO Systems Inc. solves the constrained optimization problem [58]. Figure 3.4 shows a snapshot of this optimization software package. LINGO is a tool for solving both linear and non-linear optimization problems. Branch-and-bound type techniques cannot be directly applied

unless the problems are convex. LINGO has a direct solver, a linear solver, a non-linear solver and a branch-and-bound manager. If integer restrictions exist in the problem, the software invokes a branch-and-bound manager, which in turn invokes a linear or non-linear solver, depending on the nature of the formulation. LINGO uses the revised simplex method for its linear solver, and successive linear programming, as well as a generalized reduced gradient for its non-linear solver. LINGO can solve problems with unlimited constraints and variables but cannot handle complex numbers; it requires a reformulation of the problem associated with this research work. The formulation is input in the format desired by the software. The direct solver first computes the values for as many unknown variables as possible, and if, at that stage all unknown variables are calculated, then the solution report is displayed.

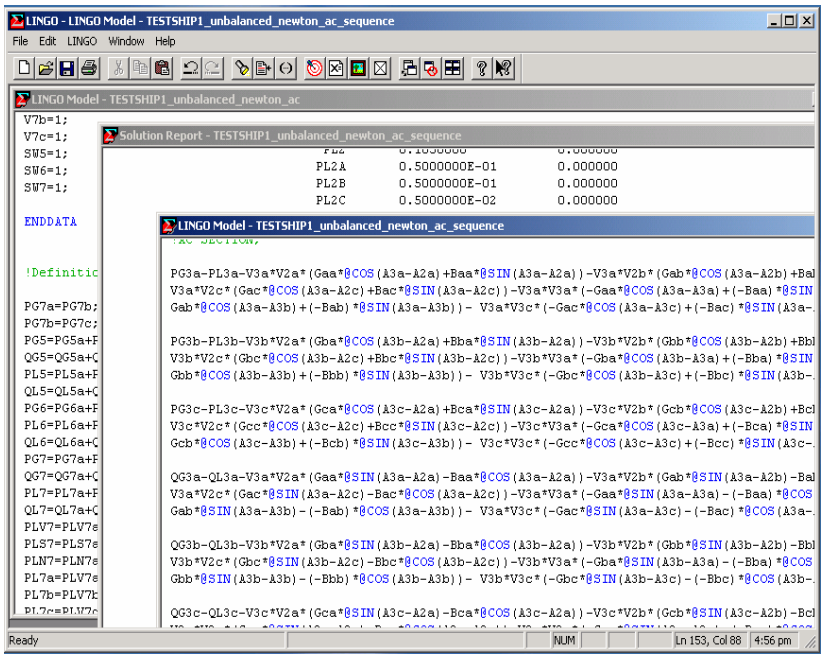

Figure 3.4: Snapshot of LINGO

If unknown variables still exist, then LINGO calls other solvers based on the model equations. If the model is continuous and linear, LINGO calls the linear solver. If the problem involves non-linear constraints, LINGO calls the non-linear solver. In case of integers, the branch-and-bound manager is called. LINGO's solver status window gives a count of the linear and non-linear variables and constraints in a model. If there are any non-linear variables in the model, the non-linear solver runs, which is slower. However, upper and lower bounds on the variables can be provided for an efficient search by using the command:

@BND(Lowerbound, Variable, Upperbound).

If the variable takes positive and negative values, it should be specified using

@FREE(Variable).

Conditional statements like “if” can also be defined:

@IF(logical_condition, true_result, false_result).

Table 3.1 displays mathematical functions with functional descriptions and Table 3.2 displays logical operators.

Table 3.1: LINGO Functions

Mathematical Functions	
@LOG(X)-returns natural logarithm	@ABS(X)-returns absolute
@TAN(X)-returns tangent	@COS(X)-returns cosine
@SIGN(X)-returns –1 if X<0 and vice-versa	@EXP(X)-returns e raised to power X
@SIN(X)-returns sine	@FLOOR(X)-rounds to lower integer
@SMAX(X1, X2,..., XN)-returns maximum value	@SQR(X)-returns square of X
@SMIN(X1, X2,..., XN)-returns minimum value	@SQRT(X)-returns square root of X

Table 3.2: LINGO Logical Functions

Logical Operators								
#NOT#	#EQ#	#NE#	#GT#	#GE#	#LT#	#LE#	#AND#	#OR#

LINGO also supports links to any DBMS for reading and writing data that has an Open Database Connectivity (ODBC) driver. LINGO can install ODBC drivers for the following DBMSs:

- Access
- dBase
- Excel
- FoxPro
- Oracle
- Paradox
- SQL Server
- Text Files

The constrained optimization problem formulated here uses non-linear and integer solvers of the LINGO software. Branch and bound guarantees optimal solution.

3.4.3 RDAP

RDAP is a software package developed by WH Power Consultants [59]. Figure 3.5 shows a snapshot of RDAP. RDAP models all three phases of a distribution system with any degree of unbalance. The program has a user interface with menu options for performing power flow, motor starting or short circuit analysis. RDAP can model:

- System: A system of substations and their associated feeders.
- Feeder: A wye or delta connected feeder

- Segment: Three-phase, two-phase or single-phase overhead or underground line defined by its end nodes, length and the Z-Model.
- Node: An end point segment.
- Load: Spot Loads and distributed loads with wye or delta connections can be modeled.
- Voltage regulators: Single-phase or three-phase with tap positions ranging from –16 to +16 can be modeled.
- Shunt Capacitors: Shunt capacitors with wye or delta connections can be modeled by specifying the MVAR rating.
- Transformers: Wye-Wye and delta-delta transformers can be modeled.

The results of power flow generated using RDAP include:

- Summary: Gives summary of input power, load power losses and shunt capacitance.
- Node Voltages Power Flow: Gives node voltages, line flows and losses at each node.
- Voltage Regulators: Gives the location, tap positions, and compensator settings for all regulators.
- Under/Over voltage: Lists all nodes operating above or below specified limits.

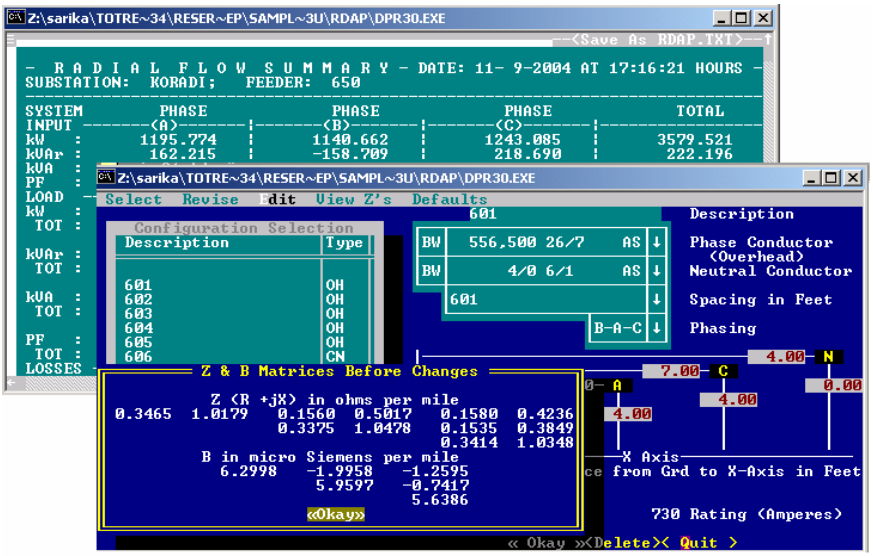

Figure 3.5: Snapshot of RDAP

3.5 Summary

This chapter introduced the two problems addressed by this research work. The traditional Healy ship system and the zonal ship system architecture are also shown. Three different software packages were used for this research. The software packages were described along with their functions and facilities. Using the tools and test systems described previously, this dissertation describes two related efforts to extend the state-of-the-art research for power systems.

Chapter 4 will describe the formulation of the equations and constraints for restoration of an unbalanced power system including DG. This work is implemented and tested on multiple terrestrial and shipboard systems demonstrating optimal restoration including islanding and load shedding.

Chapter 5 details the development of an improved algorithm to include the multiple DGs in unbalanced distribution system power flow. As part of the formulation, two types of DG models: PV and PQ are included into the algorithm. The algorithm was implemented in MATLAB and tested on multiple terrestrial and ship systems.

CHAPTER IV

OPTIMIZED RESTORATION OF UNBALANCED POWER SYSTEMS AND SHIPBOARD POWER SYSTEMS

4.1 Introduction

As discussed in Chapter 2, several techniques have been used for restoration. However, SPS have a tightly coupled structure, due to the low impedance of the cables. The power flow analysis of a SPS shows that the voltages at the nodes are approximately equal with similar voltage angles. This analysis will be further discussed in Chapter 5. Because of this nature, the fault currents are very high, thus necessitating a fast and efficient restoration scheme. The order of switching does not matter for a SPS as the system rarely loses synchronism, and returns to the nominal voltage value. This chapter deals with the restoration of SPS with IPS, i.e. the system is both AC and DC as presented in [60] and shown in detail here. The changes required with the incorporation of DG in the SPS are also stated. Thus the network reconfiguration problem is formulated as an optimization problem. The solution of the optimization formulation determines the most suitable switch operations involved in the reconfiguration. The formulation leads to a solution that does not violate any of the system constraints. Restoring vital loads first is required. Thus there are two different objectives to be satisfied. Multiobjective functions

cannot be formulated in LINGO software, and hence the objectives need to be combined into a single objective function. The single objective is to maximize the amount of power supplied to the de-energized area, while at the same time maximizing the supply of power to vital and semi-vital loads.

For the unbalanced TDS, the problem is the same: maximizing the supply to out-of-service loads. Unbalanced TDS have mutually coupled cables and different loadings in all three phases, leading to unbalanced voltages and currents, unlike the SPS. Also, terrestrial distribution systems cannot be operated looped, since the protection strategies designed for distribution systems may fail to function under these conditions. The R/X ratio of the terrestrial distribution systems is large, causing differences in power flow equations embedded as equality constraints from SPS. The power flow equations of SPS, when applied to terrestrial systems, fail to converge, as shown in [61] and detailed here. This makes the problem very different from the SPS restoration problem. The optimization problems for both SPS and terrestrial distribution systems are formulated in the next two sections.

4.2 Formulation for SPS

The problem is formulated as a mixed integer non-linear optimization problem with an objective that is subject to several constraints. As discussed previously, in the objective function, the contribution of high priority loads must be greater than the contribution of low priority loads. The loads are multiplied by a weighting factor $W^{'}$

$$W^{'}_{NVL} = 1$$
$$W^{'}_{VL} > W^{'}_{SVL} \qquad (4.1)$$

where a NVL is a Non-Vital Load, a VL is a Vital Load and a SVL is a Semi-Vital Load.

The weighting factor is selected so that the vital and semi-vital load contributions are greater than the largest non-vital load contribution. The constraints enforced on the solution are the power flow, generator limiting, load limiting, line limiting and voltage limiting constraints. There is a separate set of equality constraints for the DC side of the power system. The real power drawn from the DC side of the bus is taken to be equal to the real power delivered from the AC side. If the system is islanded, the objective is to maximize the restoration of priority loads and to shed other loads if necessary. In this formulation, some of the constraints have been formulated as binary variables, and the objective uses continuous variables.

Objective

$$Max \sum_{i \in L} W_{VL}^{'} S_{VL_i} + W_{SVL}^{'} S_{SVL_i} + W_{NVL}^{'} S_{NVL_i} \tag{4.2}$$

subject to

AC Constraints

Equality Constraints

$$PG_i - PD_i = \sum_j V_i V_j Y_{ij} \cos(\theta_{ij} + \delta_j - \delta_i) \tag{4.3}$$

$$QG_i - QD_i = \sum_j V_i V_j Y_{ij} \sin(\theta_{ij} + \delta_j - \delta_i) \tag{4.4}$$

Inequality Constraints

$$PG_i^{\min} \le PG_i \le PG_i^{\max} \tag{4.5}$$

$$QG_i^{\min} \le QG_G \le QG_{Gi}^{\max} \tag{4.6}$$

$$PL_i \le PL_i^{max} * SW_i, \text{ For Variable Load} \quad (4.7)$$

$$PL_i = T_i * PL_i^{max} * SW, \text{ For Fixed Load} \quad (4.8)$$

$$I_{ij} \le I_{ij}^{max}, \text{ Line Limits} \quad (4.9)$$

$$V_i^{min} \le V_i \le V_i^{max}, \text{ Voltage Limits} \quad (4.10)$$

$$\delta_i^{min} \le \delta_i \le \delta_i^{max}, \text{ Angle Limits} \quad (4.11)$$

DC Constraints

Equality Constraints

$$\sum_i I_{in_i} = \sum_i I_{out_i} + IL_i \qquad \begin{matrix} i \in FN \\ j \in TN \end{matrix} \quad (4.12)$$

$$V_i = V_j + I_{ij} * Z_{ij}$$

$$PL_i = T_i * PL_i^{max} * SW_i, \text{ For Fixed Load} \quad (4.13)$$

Inequality Constraints

$$PL_i \le PL_i^{max} * SW_i, \text{ For Variable Load} \quad (4.14)$$

$$I_{ij} \le I_{ij}^{max}, \text{ Line Limits} \quad (4.15)$$

$$V_i^{min} \le V_i \le V_i^{max}, \text{ Voltage Limits} \quad (4.16)$$

Switching Constraints

$$SW_i = 1, \text{ If Switch 'i' is closed}$$

$$SW_i = 0, \text{ If Switch 'i' is open} \quad (4.17)$$

$$SW_i + SW_j = 1 \qquad \begin{matrix} i \in PS \\ j \in SS \end{matrix}$$

Islanding

Objective

$$Max \sum_{i \in N_p} PL_i \tag{4.18}$$

where,

PG and QG are the real and reactive power generation

PD and QD are the real and reactive power demand

V_i is the voltage at bus i

δ_i is the angle associated with the voltage at bus i

Y_{ij} is the element of the bus admittance matrix

θ is the angle associated with Y_{ij}

PL_i is the load at bus i

T_i is the binary variable, 0 or 1

I_{ij} is the current flow from bus i to bus j

I_{in_i} and I_{out_i} are the currents entering and leaving bus i

FN is a set of from buses

TN is a set of to buses

Z_{ij} is the impedance of branch ij

PS is the set of port side switches

SS is the set of starboard side switches

N_p is the set of priority loads

Equations 4.2-4.18 in LINGO syntax are input to the software, along with the system data.

4.3 Formulation for Terrestrial Unbalanced Distribution Systems

This section presents two different formulations for the problem. The first formulation utilizes Newton equations as equality constraints, and the second formulation utilizes the nodal current and voltages. The first formulation utilizes real power and reactive power and is highly non-linear as compared to the second formulation that utilizes voltage and current.

4.3.1 Formulation I

Objective

$$Max \sum_{i \in L} W_{VL}^{'} S_{VL_i} + W_{SVL}^{'} S_{SVL_i} \tag{4.19}$$

subject to

Equality Constraints

$$S_i^p = P_i^p + jQ_i^p \tag{4.20}$$

$$P_i^p = \left|V_i^p\right| \sum_{k=1}^{n} \sum_{m=a}^{c} \left|V_k^m\right| \left[G_{ik}^{pm} \cos\theta_{ik}^{pm} + B_{ik}^{pm} \sin\theta_{ik}^{pm}\right] \tag{4.21}$$

$$Q_i^p = \left|V_i^p\right| \sum_{k=1}^{n} \sum_{m=a}^{c} \left|V_k^m\right| \left[G_{ik}^{pm} \sin\theta_{ik}^{pm} - B_{ik}^{pm} \cos\theta_{ik}^{pm}\right] \tag{4.22}$$

$$PL_i = PL_i^{\max} * T_i^p \text{, For Fixed Load} \tag{4.23}$$

Inequality Constraints

$$P_{Gi}^{\min} \le P_{Gi} \le P_{Gi}^{\max} \text{, Generator Real Power Limit} \tag{4.24}$$

$$Q_{Gi}^{\min} \le Q_{Gi} \le Q_{Gi}^{\max} \text{, Generator Reactive Power Limit} \tag{4.25}$$

$$I_{ij}^p \le I_{ij,\max}^p \text{, Line Limits} \tag{4.26}$$

$$V_{i,\min}^{p} \le V_{i}^{p} \le V_{i,\max}^{p}, \text{ Voltage Magnitude Limits} \quad (4.27)$$

$$\delta_{i,\min}^{p} \le \delta_{i}^{p} \le \delta_{i,\max}^{p}, \text{ Voltage Angle Limits} \quad (4.28)$$

where

$p \in$ set of phases a, b and c and $L \in$ set of load nodes.

P_i^p and Q_i^p are the net active and reactive power injections in phase p of node i.

S_i is the three-phase apparent power.

V_i^p is the voltage of phase p of node i.

G_{ik}^{pm} and B_{ik}^{pm} are the real and reactive parts of the 3×3 admittance matrix (Y) of branch between node i and node k

θ_{ik}^{pm} is the difference in voltage angle between phases p and m of nodes i and k.

T_i^p is a binary variable.

$W_{VL}^{'}$ is weighting factor for a vital load that is greater than the weighting factor for a semi-vital load ($W_{SVL}^{'}$).

The model was first tested on a small unbalanced system shown in Figure 4.1 and the results are shown in Table 4.1. All switches are in a closed position, and the steady state solution is obtained by optimization. This steady state solution is thus a power flow solution.

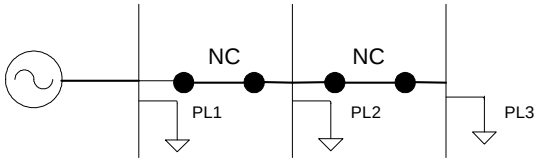

Figure 4.1: Test Case

When this formulation was used for restoration of systems with the number of nodes larger than four, the solution failed to converge. This failure to converge is attributed to the fact that distribution systems are ill-conditioned systems, and thus the Jacobian became singular. A decoupling procedure was also tried, which split the problem into two sub problems *P-θ* and *Q-V*, but due to the high *R/X* ratio of the lines, it still failed to converge. Other decoupling methods exist [62, 63] that show convergence even for an R/X ratio as high as 2.

Table 4.1: Results for Test Case

Load PL	Vital a	Vital b	Vital c	Semi Vital a	Semi Vital b	Semi Vital c	Switch position	Total Gen a	Total Gen b	Total Gen c
1	1	0.1	0.1	0	0	0	SW1 closed	6.501	1.101	0.212
2	0	0	0	0.5	0.5	0.05	SW2 closed			
3	0	0	0	5	0.5	0.05	SW3 closed			

4.3.2 Formulation II

To counter the issues with the previous algorithm, a new algorithm was formulated. First, component models for the distribution system were obtained. These components are the cables, loads and distributed loads. The models of these components are developed in Chapter 5.

Objective

$$Max \sum_{i \in L} IL_i^p + W_s' \left(\sum_{i=1}^{m} CS_i + \sum_{j=1}^{n} \left(1 - OS_j\right) \right) \tag{4.29}$$

subject to

Equality Constraints

$$V_j^p = SW_{ij}\left(V_i^p - \sum_{m=a}^{c} Z_{ij}^{mp} I_{ij}^p\right) + slack_{ij}^p\left(1 - SW_{ij}\right) \quad (4.30)$$

$$\sum_N I_{ij}^p - \sum_O I_{jr}^p - IL_j^p = 0 \quad (4.31)$$

$$I_{ij}^p = SW_{ij} * slackcurr_{ij}^p \quad (4.32)$$

$$IL^p = T_i^p * IL_{i,\max}^p, \text{ For Fixed Load} \quad (4.33)$$

Inequality Constraints

$$V_{i,\min}^p \le V_i \le V_{i,\max}^p, \text{ Voltage Magnitude Limits} \quad (4.34)$$

$$IL_i^p \le IL_{i,\max}^p, \text{ For Variable Load} \quad (4.35)$$

$$I_{ij}^p \le I_{ij,\max}^p, \text{ Line Limits} \quad (4.36)$$

where,

CS is the closed switch

OS is the open switch

IL_i^p is the load current flowing in phase p of node i

$W_s^{'}$ is the weighting factor which is less than 1

SW_{ij} is the switch between nodes i and j.

Z_{ij}^{mp} is mutually coupled 3×3 impedance matrix of the branch between nodes i and j.

T_i^p is a binary variable.

N is the set of branches with currents going into the node j

O is the set of branches with currents coming out of the node j.

Equations (4.37) and (4.38) are the governing equations of the voltage at a node j in Figure 4.2 that can be fed by two branches depending on which switch is closed. The second term on the right hand side of (4.30) is added to (4.37) and (4.38) in order to validate both equations simultaneously.

$$V_j = SW_{ij}\left(V_i - Z_{ij} I_{ij}\right) \tag{4.37}$$

$$V_j = SW_{kj}\left(V_i - Z_{kj} I_{kj}\right) \tag{4.38}$$

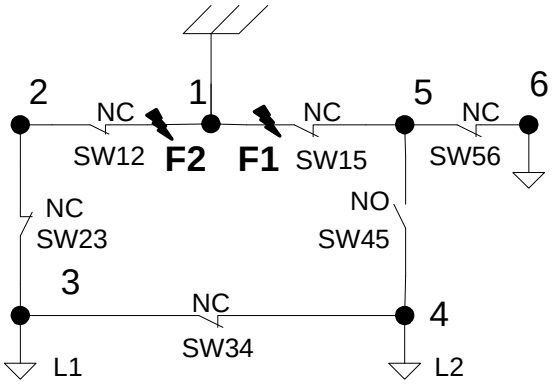

Figure 4.2: Illustration of Switch Pairs

The fault is detected and isolated before performing restoration. This is simulated by setting the corresponding $SW_{ij} = 0$ and thereby $I_{ij} = 0$. The variable *slackcurr* ensures that (4.31) is valid when $SW_{ij} = 0$. Since the problem becomes difficult to solve with the increasing size of the system, two types of switching schemes are considered:

A. Schemes

Two schemes, viz. the "with switch pairs scheme" (WSPS) and "without switch pairs scheme" (WOSPS), are considered. For the WSPS, an additional constraint (4.39) is

introduced in formulation II. This additional constraint automatically takes care of radiality as only one of the two switches will be closed at a given time.

$$SW_{ij} + SW_{kj} = 1 \; \forall ij \text{ and } jk \in SP \tag{4.39}$$

SP is the set of switches that make switch pairs. No radiality constraint needs to be enforced, as the system is always radial. For the WOSPS radiality constraint (4.40) is added to formulation II.

$$\sum_{i \in SL} SW_i \leq n-1 \tag{4.40}$$

SL is the set of switches that result in a loop. WSPS involves a search space of solutions smaller than WOSPS. However, WSPS fails to provide a restoration scheme for several faults as shown in Figure 4.2. For a fault F1, with SW15 and SW45 as a pair, the restoration path to L3 is through SW12-SW23-SW34-SW45 and SW56. For the same switch pair and a fault at F2, there is no restoration path to L1 and L2. The WSPS scheme needs no additional radiality constraint to be reinforced; the search space of solutions is small, but it fails to provide a restoration path even if one exists for some problems. The WOSPS scheme needs the enforcement of the radiality constraint; its search space of solutions is large, but it provides a restoration path for all faults if one exists. This distinction shows a clear trade off between both schemes.

B. Formulation in LINGO

Formulation II requires the solution of a mixed-integer non-linear optimization problem for which LINGO is used. LINGO does not have a facility for complex numbers and hence the problem is subdivided into real and imaginary sub problems.

$$Max \sum_{k \in PS} \left(IL_k^p R + IL_k^p I \right) + \sum_{k \in NG} \left(\left(1 - IL_k^p R\right) + \left(1 - IL_k^p I\right) \right) + W_s \left(\sum_{i=1}^{m} CS_i + \sum_{j=1}^{n} \left(1 - OS_j\right) \right) \tag{4.41}$$

subject to

Equality Constraints

$$V_j^p R = SW_{ij} \left(V_j^p R - \sum_{m=a}^{m=c} Z_{ij}^{mp} R * I_{ij}^{mp} R \right) + slack_{ij}^p R \left(1 - SW_{ij}\right) \tag{4.42}$$

$$V_j^p I = SW_{ij} \left(V_j^p I - \sum_{m=a}^{m=c} Z_{ij}^{mp} I * I_{ij}^{mp} I \right) + slack_{ij}^p I \left(1 - SW_{ij}\right) \tag{4.43}$$

$$\sum_i I_{ij}^p R - \sum_r I_{jr}^p R - IL_j^p R = 0 \tag{4.44}$$

$$\sum_i I_{ij}^p I - \sum_r I_{jr}^p I - IL_j^p I = 0 \tag{4.45}$$

$$I_{ij}^p R = SW_{ij} * slackcurr_{ij}^p R \tag{4.46}$$

$$I_{ij}^p I = SW_{ij} * slackcurr_{ij}^p I \tag{4.47}$$

$$V_i^p - \left(V_i^p R * V_i^p R + V_i^p I * V_i^p I \right)^{0.5} = 0 \tag{4.48}$$

$$I_i^p - \left(I_i^p R * I_i^p R + I_i^p I * I_i^p I \right)^{0.5} = 0 \tag{4.49}$$

$$I_{ij}^p - \left(I_{ij}^p R * I_{ij}^p R + I_{ij}^p I * I_{ij}^p I \right)^{0.5} = 0 \tag{4.50}$$

$$IL_i^p R = T_i^p R * IL_{i,\max}^p R \tag{4.51}$$

$$IL_i^p I = T_i^p I * IL_{i,\max}^p I \tag{4.52}$$

Inequality Constraints

$$V_{i,\min}^p \le V_i^p \le V_{i,\max}^p \text{, voltage magnitude limits} \tag{4.53}$$

$$\begin{aligned} IL_i^p R &\le IL_{i,\max}^p R \\ IL_i^p I &\le IL_{i,\max}^p I \end{aligned} \quad (IL_i^{Ph} R) \text{ and } (IL_i^{Ph} I) > 0 \text{, for variable load} \tag{4.54}$$

$$\begin{matrix} IL_i^p R \geq IL_{i,\max}^p R \\ IL_i^p I \geq IL_{i,\max}^p I \end{matrix} \quad (IL_i^{Ph} R) \text{ and } (IL_i^{Ph} I) < 0 \text{, for variable load} \tag{4.55}$$

$$I_{ij}^p \leq I_{ij,\max}^p \text{, line limits} \tag{4.56}$$

$$\sum_{i \in SL} SW_i \leq n-1 \text{, for the WOSPS scheme} \tag{4.57}$$

$$SW_{ij} + SW_{jk} = 1 \text{, for the WSPS scheme} \tag{4.58}$$

where

PS are the set of loads with positive real and imaginary parts

NG are those sets with negative real and imaginary parts

The results in the next section will validate this formulation.

4.4 Test Cases Description

This section describes the test cases to demonstrate restoration along with some of the data.

4.4.1 SPS

The model of the SPS shown in Figure 4.3 uses a 4-zone topology with two Ship Service Converter Modules serving loads in each zone. The system is essentially radial, as radial distribution networks have a significant advantage over meshed networks. These advantages are lower short circuit currents, simpler switching and easy design of protective equipment and its coordination. However, radial structure provides lower reliability. In order to increase reliability, DG can be employed. The AC generator is in zone-4. However, a DG is also in zone-1. AC to DC rectifiers are in zones 1 and 4. Vital

and semi-vital loads are provided with an alternative path using ABT, which switches between the port and starboard buses.

Figure 4.4 shows details of each load center. Each load center has a vital, semi-vital and a non-vital load. The ABT uses two switches in this model; only one of these switches is in the closed position at a certain time. Since the objective is a maximization function, all vital and semi-vital loads will be attempted to be restored first.

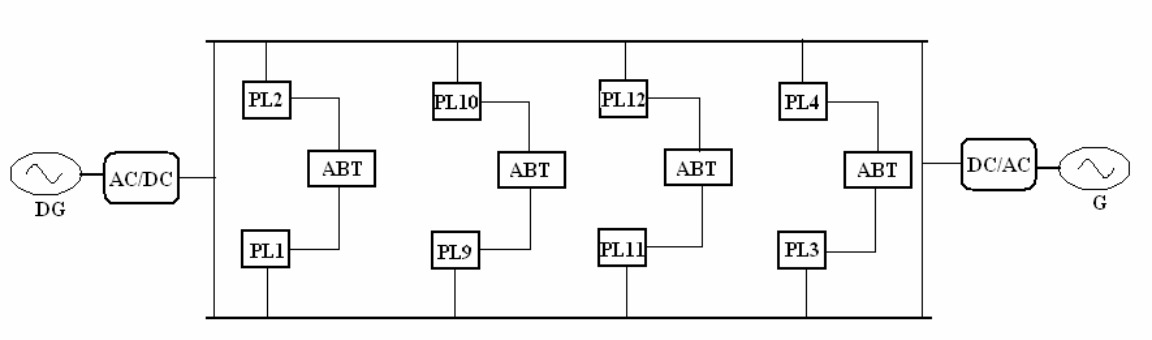

Figure 4.3: SPS Model

Table 4.2 shows data of the SPS generated using the data given in reference [64]. The total load of the system is 10 MW. The generator can generate up to 8 MW. The DG has, however, less capacity and can only generate up to 4 MW.

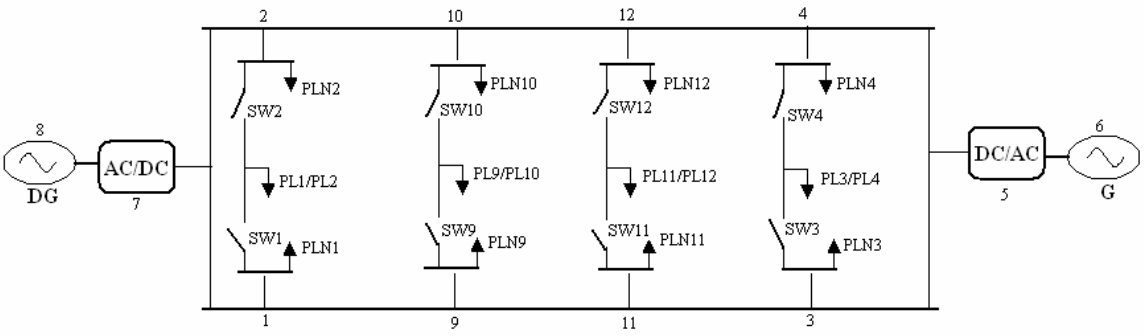

Figure 4.4: Detailed Topology of SPS

Table 4.2: SPS Data

Total Load	0.025*4=0.1pu=10 MW
Gen1 capacity	0.08 pu = 8 MW
DG capacity	0.04 pu = 4 MW

4.4.2 IEEE 13-Node Feeder

The data for this test was obtained from the IEEE test case archive for distribution feeders [65]. The layout of the feeder is shown in Figure 4.5. The data is characterized by:

Loads – Spot loads and distributed loads, single-phase and three-phase balanced and unbalanced loads, wye and delta connected, constant kW, kVAR, constant Z and constant I type.

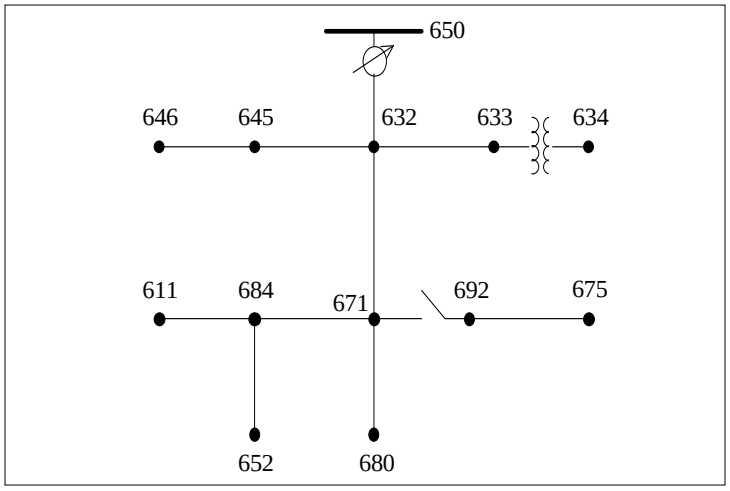

Figure 4.5: IEEE 13-Node Feeder

Overhead and Underground Lines – Three-phase and single-phase lines with different spacings of phases.

Transformer – A substation transformer is a delta-grounded wye connection and an inline transformer is a grounded wye-grounded wye connection.

Capacitor - Balanced three-phase capacitor and single-phase capacitor

4.4.3 IEEE 37-Node Feeder

The IEEE 37-node feeder is an actual feeder in California. The feeder was analyzed for which the data was also obtained from IEEE test case archive for distribution feeders. The layout of the feeder is shown in Figure 4.6. The data is characterized by:

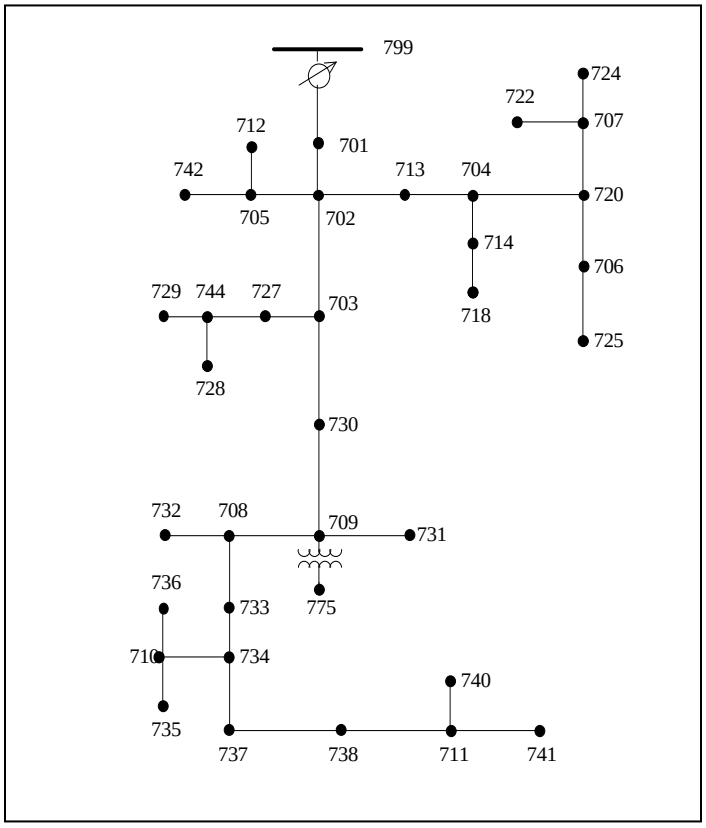

Figure 4.6: IEEE 37-Node Feeder

Loads – Spot loads, single-phase and three-phase balanced and unbalanced loads, delta connected, constant kW, kVAR, constant Z and constant I type.

Overhead and Underground Lines – Three-phase lines with different spacing of phases.

Transformer – Substation transformer and inline transformer is delta-delta.

4.5 Results of Restoration for SPS

The optimization formulation in Section 4.1 was used to reconfigure the SPS under fault conditions. The pre-fault system conditions are as shown in Table 4.3. Equating the respective variable to zero simulates a fault. The variable is equated to zero because if there is a fault in any part, that part of the ship is not available. Because of the fault and the isolation of the fault, some loads will be left without any supply. Affected loads need to have their power restored.

Consider Scenario 1, where faults occur on lines 2-10 and 4-12, as shown in Figure 4.7. This fault leads to loss of non-vital loads PLN10 and PLN12. No restoration path is available for these loads, so there is no switching and the DG ramps down to 1.38 MW due to loss of two non-vital loads. The configuration after restoration is as shown in Table 4.4. Consider Scenario 2, where faults occur on lines 2-10 and 3-11. An alternate path is available to the vital and semi-vital loads left unrestored after the clearance of the fault. The configuration after restoration is as shown in Table 4.5. Now consider scenario 3, where faults occur on lines 4-12 and 3-11. Many priority loads are lost, and no other alternative path is available from the generator, under such a fault scenario.

Table 4.3: Pre-Fault Configuration

Load PL	Vital (MW)	Semi-Vital (MW)	Non-Vital at PB (MW)	Non-Vital at SB (MW)	Switch position	Total Generation Gen	DG
Load 1/2	0.5	1	0.5	0.5	SW1 closed	7.33 MW	2.95 MW
Load 3/4	0.5	1	0.5	0.5	SW4 closed		
Load 9/10	0.5	1	0.5	0.5	SW9 closed		
Load 11/12	0.5	1	0.5	0.5	SW11 closed		

Now the DG, which was only supplying some part of the load in normal conditions (without fault) ramps up. Since islanding is taking place, only priority loads are restored, and the rest of the loads are shed. The after-fault scenario is as shown in Table 4.6. The DG ramps to maximum output power, i.e., 4 MW and supplies priority loads in zones 1, 2 and 3. This action creates an island supplied by DG, as shown in Figure 4.8. However, the main generator continues to supply the load in Zone-4.

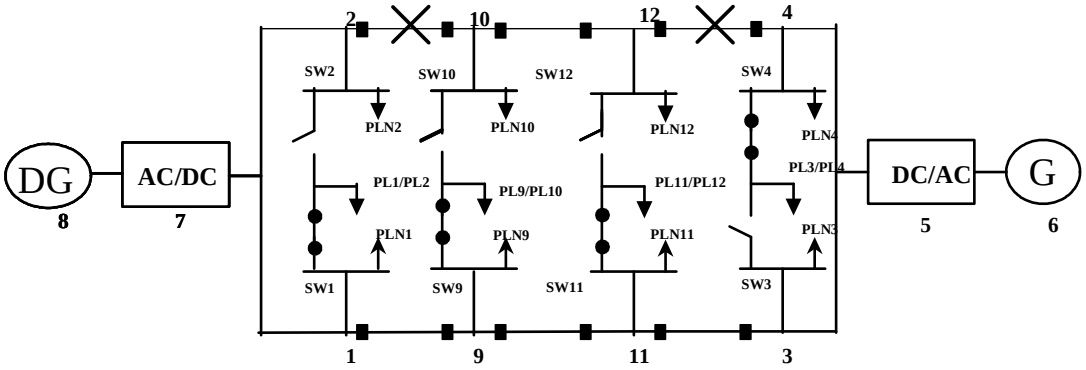

Figure 4.7: SPS Fault-Scenario 1

Table 4.4: After Restoration Configuration - Scenario 1

Load PL	Vital (MW)	Semi-Vital (MW)	Non-Vital at PB (MW)	Non-Vital at SB (MW)	Switch position	Total Generation Gen	DG
Load 1/2	0.5	1	0.5	0.5	SW1 closed	7.33 MW	1.38 MW
Load 3/4	0.5	1	0.5	0.5	SW4 closed		
Load 9/10	0.5	1	0.0	0.5	SW9 closed		
Load 11/12	0.5	1	0.0	0.5	SW11 closed		

Table 4.5: After Restoration Configuration - Scenario 2

Load PL	Vital (MW)	Semi-Vital (MW)	Non-Vital at PB (MW)	Non-Vital at SB (MW)	Switch position	Total Generation Gen	DG
Load 1/2	0.5	1	0.0	0.0	SW1 closed	6.87 MW	3.6 MW
Load 3/4	0.5	1	0.5	0.5	SW4 closed		
Load 9/10	0.5	1	0.5	0.5	SW10 closed		
Load 11/12	0.5	1	0.5	0.5	SW12 closed		

Table 4.6: After Restoration Configuration - Scenario 3

Load PL	Vital (MW)	Semi-Vital (MW)	Non-Vital at PB (MW)	Non-Vital at SB (MW)	Switch position	Total Generation Gen	DG
Load 1/2	0.5	1	0.0	0.0	SW1 closed	2.54 MW	4.00 MW
Load 3/4	0.5	1	0.5	0.5	SW3 closed		
Load 9/10	0.5	0.76	0.0	0.0	SW10 closed		
Load 11/12	0.5	0.74	0.0	0.0	SW11 closed		

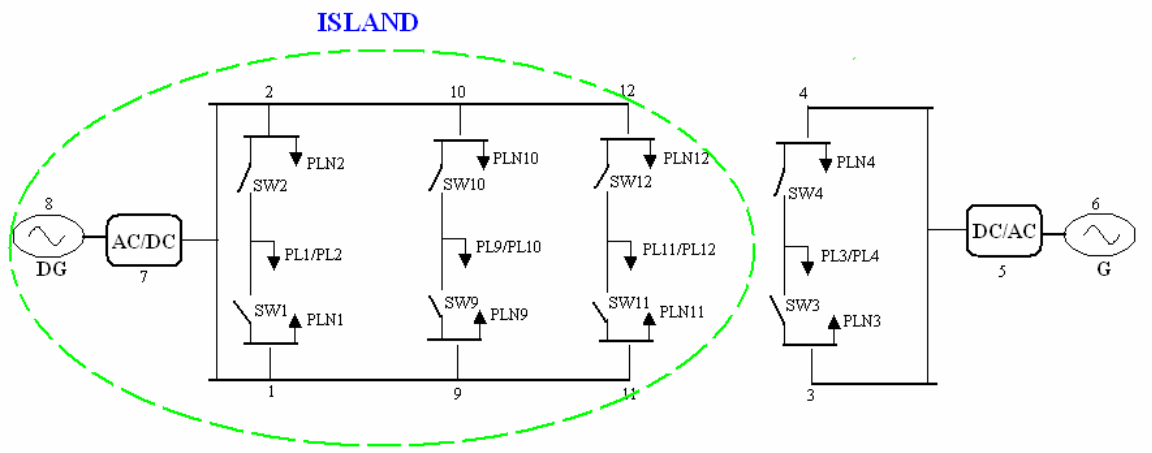

Figure 4.8: After Restoration-Scenario 3

4.6 Results of Restoration for Unbalanced Terrestrial Distribution Systems

The SPS considered in the previous section was balanced. In this section unbalanced systems, i.e. IEEE 13-node and IEEE 37-node systems, introduced in

Sections 4.4.2 and 4.4.3 are considered.

4.6.1 IEEE 13-Node System

IEEE 13-node distribution system is considered first, and some assumptions are made:

1. The regulator is removed from the system
2. Capacitors are not modeled and hence they are removed from the system.
3. A dummy node "7" is introduced due to distributed load modeling.
4. Steps 1 and 2 lead to lower and unacceptable voltages in the system. The load is reduced to bring the voltages within limits of 0.95 and 1.05.
5. All loads are considered as constant current loads.
6. Normally open tie switches are introduced in the system for creating restoration scenarios.

As shown in Figure 4.9, a switch is introduced in each branch. Three normally open switches and thirteen normally closed switches are in the system. Initially, optimization is run under an unfaulted condition, for the configuration of switches as shown in Figure 4.9. Keeping all the switches closed with no switching finds the steady state solution. The steady state solution obtained by the optimization software is compared with the developed unbalanced power flow program described in Chapter 5 and developed in MATLAB [66]. A comparison of voltage magnitudes in p.u. and voltage angles in degrees, obtained from developed software and the optimization solution is shown in Table 4.7. These results demonstrate the validity of optimization formulation and that fault scenarios can now be simulated.

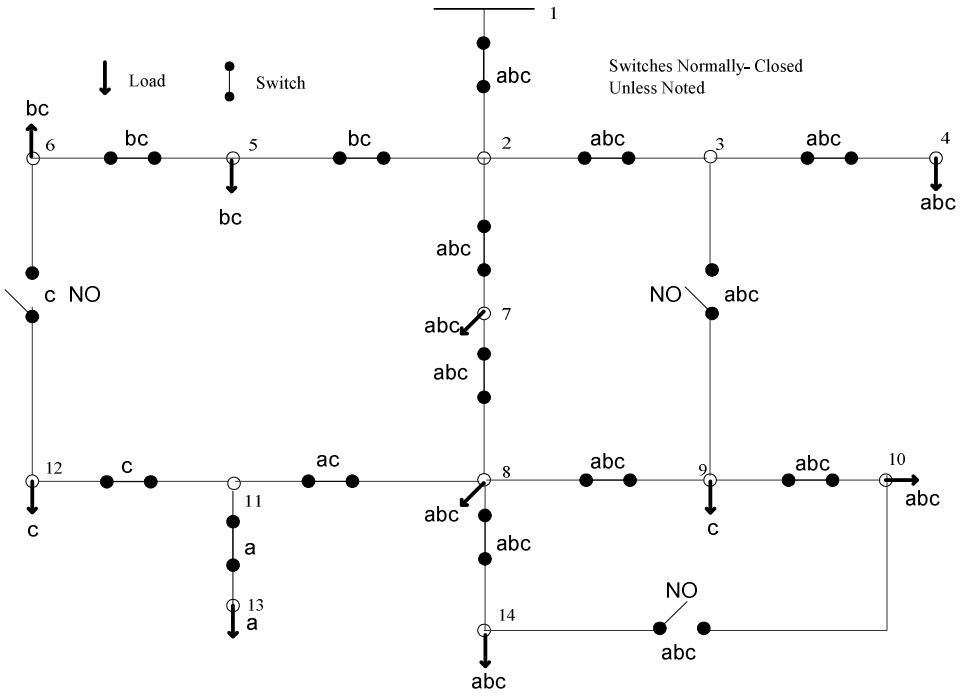

Figure 4.9: Modified IEEE 13-Node System

Table 4.7: Results Verification for Modified IEEE 13-Node System

Node ID	LINGO		MATLAB		LINGO		MATLAB		LINGO		MATLAB	
	Van	∠Van	Van	∠Van	Vbn	∠Vbn	Vbn	∠Vbn	Vcn	∠Vcn	Vcn	∠Vcn
1	1	0	1	0	1	-120	1	-120	1	120	1	120
2	0.986	-0.31	0.985	-0.4	0.99	-120.87	0.99	-120.84	0.992	119.51	0.992	119.61
3	0.982	-0.39	0.981	-0.5	0.99	-120.91	0.989	-120.88	0.991	119.54	0.991	119.65
4	0.98	-0.44	0.979	-0.5	0.99	-120.93	0.989	-120.9	0.99	119.57	0.99	119.68
5					0.983	-120.96	0.982	-120.93	0.994	119.46	0.994	119.56
6					0.981	-121	0.98	-120.97	0.995	119.44	0.994	119.54
7	0.985	-0.42	0.984	-0.5	0.991	-120.87	0.99	-120.83	0.99	119.43	0.989	119.52
8	0.981	-0.79	0.98	-0.9	0.993	-120.8	0.992	-120.77	0.983	119.27	0.982	119.37
9	0.981	-0.8	0.98	-0.9	0.993	-120.79	0.992	-120.75	0.982	119.26	0.982	119.35
10	0.981	-0.81	0.98	-0.9	0.993	-120.79	0.992	-120.75	0.982	119.26	0.982	119.35
11	0.979	-0.84	0.978	-0.9					0.981	119.28	0.981	119.37
12									0.979	119.25	0.979	119.34
13	0.972	-0.76	0.971	-0.8								
14	0.981	-0.8	0.98	-0.9	0.993	-120.8	0.992	-120.76	0.982	119.27	0.982	119.37
Voltage magnitudes are in per unit and voltage angles are in degrees												

Suppose a fault occurs on the branch 8-9, and SW89 is opened. The load at node 9, which is a single-phase load, and the load at node 10, which is a three-phase load, are left without supply. The solution obtained after optimization is to close SW1014 to supply both loads. Consider another fault at branch 2-3. After restoration for the fault at 2-3, the magnitude of current flowing in branch 3-4 was 0.5825, 0.2250, 0.2250 pu in phases a, b and c. Partial shedding of variable three-phase load 4 occurs under the same fault when the limit of cable 3-4 is reduced to 0.4, 0.2, 0.2 in a, b and c phases. Faults are simulated in several other locations. The CPU time to find a global optimal with switches whose status change after restoration are shown in Table 4.8. Since non-linear branch and bound techniques were used in LINGO coupled with the switching operations constraint, the solution is guaranteed to be an optimal solution.

Table 4.8 demonstrates that the time required to find a global optimal solution for WSPS scheme is much less than the time required for WOSPS scheme. However, WSPS scheme fails to provide a feasible solution for several fault scenarios.

Table 4.8: Restoration of Modified IEEE 13-Node System

Case ID	Case Description	WSPS		WOSPS	
		Time (Sec)	Switching	Time (Sec)	Switching
1	9-10	1	Close - 1014	62	Close - 1014
2	2-3	1	Close - 39	57	Close - 39
3	11-12	1	Close - 612	1	Close - 612
4	8-9	NSF	NSF	60	Close - 1014
5	8-9 & 2-3	NSF	NSF	1	Close - 39 and 1014
6	2-7	NSF	NSF	69	Close - 39
7	7-8	NSF	NSF	70	Close - 39
8	2-3 & decreasing cable limit on 3-4	5	Close - 39, Partial supply to variable Load 4	150	Close - 39, Partial supply to variable Load 4
NSF = No Solution Found					

A plot of voltages for some critical nodes, after the restoration for the WSPS and WOSPS schemes are shown in Figures 4.10a and 4.10b. The voltages are within the prescribed tolerances of 0.95 and 1.05.

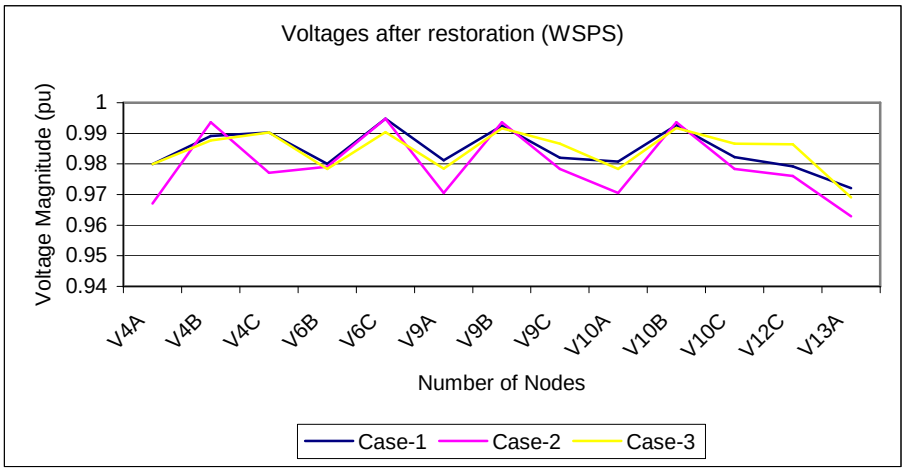

(a)

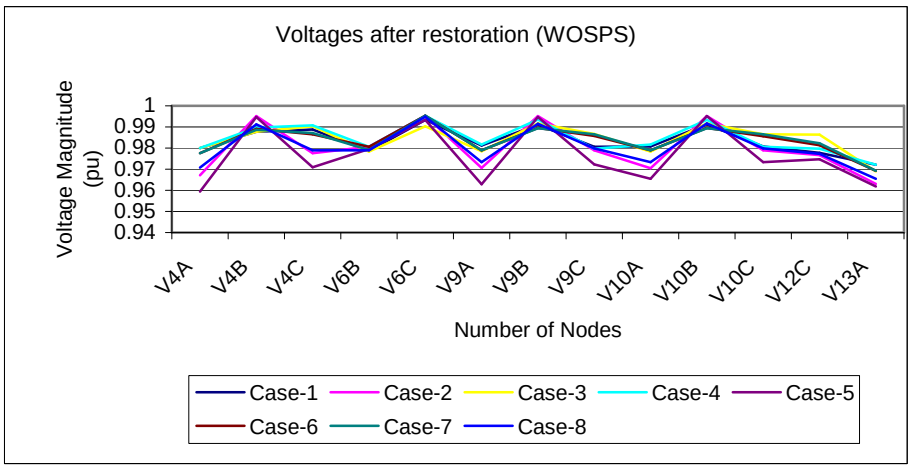

(b)

Figure 4.10: Voltages after Restoration for Modified IEEE 13-Node System

4.6.2 IEEE 37-Node System

The IEEE 37-node distribution system, which is an actual distribution system in California, was also considered and some assumptions were made:

1. Regulator was removed from the system
2. All loads were considered as constant current loads.
3. Normally open tie switches as shown in Figure 4.11 were introduced in the system for creating restoration scenarios.

There are six normally open switches and thirty-six normally closed switches. Initially, the optimization runs under unfaulted condition and for the configuration of switches as shown in Figure 4.11. The comparison of solution with a developed unbalanced power flow program in MATLAB is shown in Table 4.9.

Faults are simulated in several locations. The CPU time to find a global optimal along with switches whose status change after restoration are shown in Table 4.10. Since non-linear branch and bound techniques were used in LINGO coupled with the switching operations constraint, the solution is guaranteed to be an optimal solution. For this test case, only the switches downstream of the faulted branch are considered as variables, in addition to normally open switches. Figure 4.12 shows a plot of voltages after the restoration for some critical nodes. Since all nodes in this test system are three-phase nodes, the positive sequence voltage is plotted.

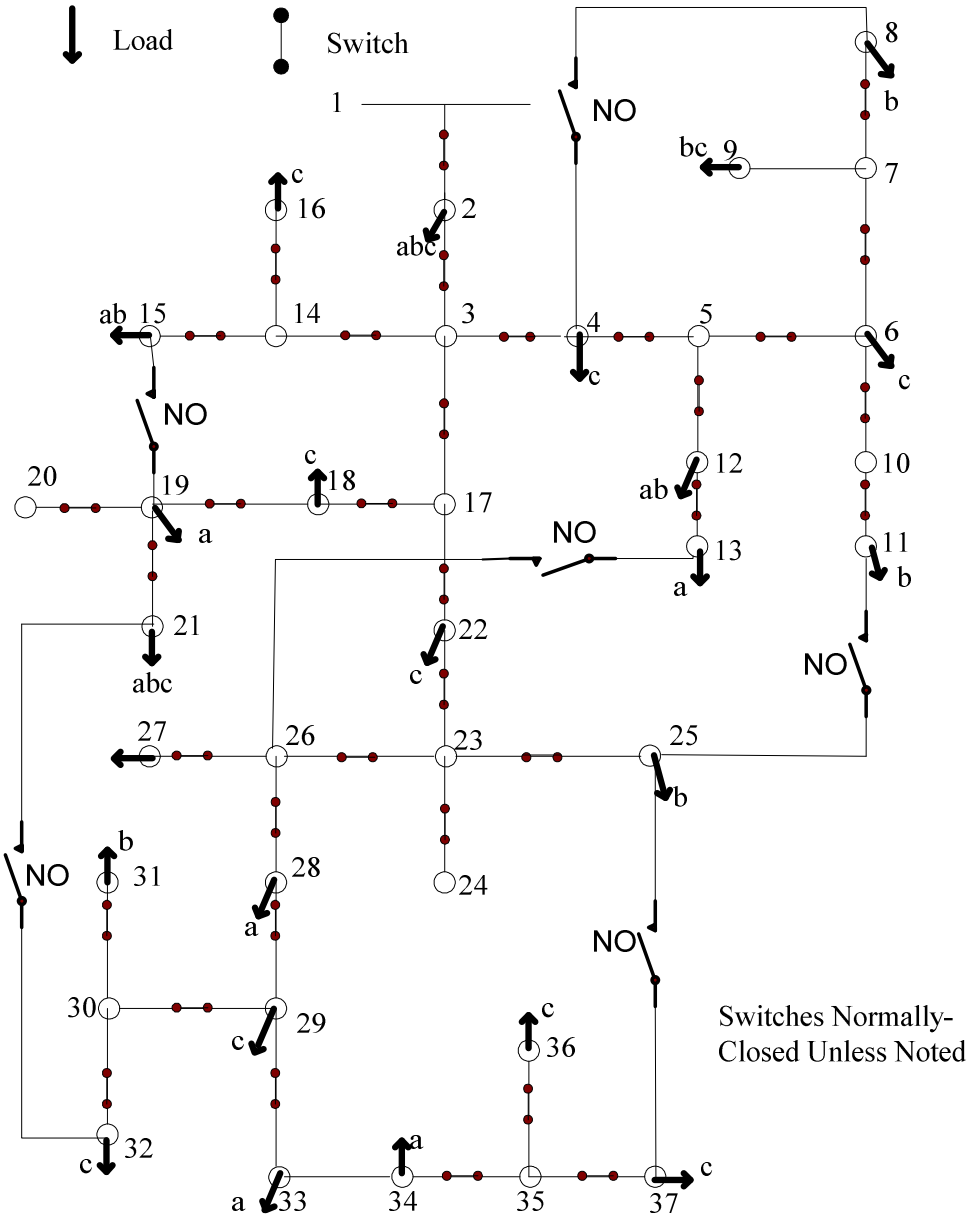

Figure 4.11: Modified IEEE 37-Node System

Table 4.9: Results Verification for Modified IEEE 37-Node

Node ID	LINGO		MATLAB		LINGO		MATLAB		LINGO		MATLAB	
	Vab	∠Vab	Vab	∠Vab	Vbc	∠Vbc	Vbc	∠Vbc	Vca	∠Vca	Vca	∠Vca
1	1	-30	1	-30	1	-150	1	-150	1	90	1	90
2	0.986	-30.17	0.985	-30.13	0.99	-150.11	0.99	-150.22	0.987	89.5	0.986	89.54
3	0.978	-30.27	0.977	-30.23	0.984	-150.21	0.985	-150.32	0.98	89.26	0.979	89.3
4	0.976	-30.26	0.975	-30.22	0.982	-150.24	0.983	-150.35	0.978	89.26	0.977	89.29
5	0.975	-30.26	0.974	-30.22	0.98	-150.27	0.981	-150.38	0.976	89.27	0.975	89.31
6	0.973	-30.22	0.972	-30.18	0.978	-150.35	0.979	-150.46	0.972	89.3	0.971	89.33
7	0.973	-30.19	0.972	-30.15	0.974	-150.44	0.974	-150.55	0.968	89.45	0.968	89.48
8	0.973	-30.19	0.972	-30.15	0.973	-150.45	0.974	-150.57	0.968	89.48	0.967	89.51
9	0.973	-30.19	0.972	-30.15	0.973	-150.44	0.974	-150.56	0.968	89.46	0.967	89.49
10	0.973	-30.22	0.972	-30.18	0.978	-150.36	0.978	-150.47	0.972	89.3	0.971	89.34
11	0.973	-30.22	0.972	-30.18	0.977	-150.37	0.978	-150.48	0.972	89.32	0.971	89.35
12	0.974	-30.26	0.973	-30.22	0.98	-150.27	0.981	-150.37	0.976	89.28	0.975	89.31
13	0.973	-30.29	0.972	-30.25	0.979	-150.22	0.98	-150.33	0.976	89.27	0.975	89.31
14	0.977	-30.24	0.976	-30.2	0.983	-150.23	0.984	-150.34	0.979	89.27	0.978	89.31
15	0.977	-30.24	0.976	-30.2	0.982	-150.24	0.983	-150.35	0.978	89.3	0.977	89.33
16	0.976	-30.22	0.975	-30.18	0.983	-150.23	0.984	-150.34	0.978	89.26	0.977	89.29
17	0.97	-30.41	0.969	-30.38	0.979	-150.24	0.98	-150.35	0.975	89.03	0.975	89.06
18	0.969	-30.41	0.968	-30.37	0.978	-150.21	0.979	-150.32	0.975	89.03	0.974	89.06
19	0.968	-30.42	0.967	-30.39	0.978	-150.2	0.978	-150.31	0.974	89.02	0.974	89.05
20	0.968	-30.43	0.967	-30.39	0.977	-150.19	0.978	-150.3	0.974	89.02	0.974	89.05
21	0.968	-30.42	0.967	-30.38	0.977	-150.2	0.978	-150.31	0.974	89.02	0.973	89.06
22	0.964	-30.42	0.963	-30.39	0.975	-150.19	0.976	-150.3	0.972	88.93	0.971	88.95
23	0.962	-30.43	0.961	-30.4	0.974	-150.17	0.975	-150.28	0.971	88.9	0.97	88.93
24	0.962	-30.43	0.961	-30.4	0.974	-150.17	0.975	-150.28	0.971	88.9	0.97	88.93
25	0.962	-30.43	0.961	-30.4	0.974	-150.19	0.974	-150.3	0.97	88.92	0.969	88.95
26	0.96	-30.45	0.959	-30.42	0.973	-150.13	0.973	-150.24	0.969	88.85	0.969	88.87
27	0.959	-30.44	0.958	-30.41	0.973	-150.13	0.973	-150.24	0.969	88.84	0.968	88.87
28	0.957	-30.47	0.956	-30.45	0.971	-150.09	0.972	-150.2	0.968	88.81	0.968	88.82
29	0.953	-30.49	0.952	-30.47	0.969	-150.04	0.969	-150.15	0.966	88.73	0.966	88.75
30	0.952	-30.45	0.951	-30.43	0.968	-150.05	0.969	-150.16	0.965	88.72	0.964	88.74
31	0.952	-30.45	0.951	-30.42	0.967	-150.08	0.967	-150.19	0.964	88.78	0.963	88.79
32	0.952	-30.43	0.951	-30.41	0.968	-150.05	0.969	-150.16	0.964	88.71	0.964	88.73
33	0.95	-30.55	0.949	-30.52	0.967	-149.97	0.967	-150.07	0.965	88.68	0.965	88.7
34	0.949	-30.55	0.948	-30.53	0.966	-149.94	0.967	-150.05	0.965	88.65	0.964	88.67
35	0.948	-30.53	0.947	-30.51	0.966	-149.94	0.967	-150.05	0.964	88.62	0.963	88.64
36	0.948	-30.51	0.946	-30.49	0.966	-149.94	0.967	-150.05	0.964	88.61	0.963	88.63
37	0.948	-30.52	0.947	-30.5	0.966	-149.94	0.967	-150.05	0.964	88.61	0.963	88.63

Table 4.10: Restoration of Modified IEEE 37-Node System

Case ID	Fault	Time Elapsed (Seconds)	Switch Status Open	Close
1	4-5	41	-	04-08
2	28-29	30	35-37	21-32, 25-37
3	22-23	91	26-28, 34-35	21-32, 11-25, 25-37, 13-26
4	17-18	3	-	15-19
5	23-26	120	29-30, 35-37	21-32, 25-37, 13-26
6	5-6 and 28-29 with cable capacity reduced on 04-08	320	6-7, 30-32	04-08, 21-32, 11-25, 25-37
7	5-6 and 28-29	11	10-11, 30-32	04-08, 11-25, 21-32, 25-37

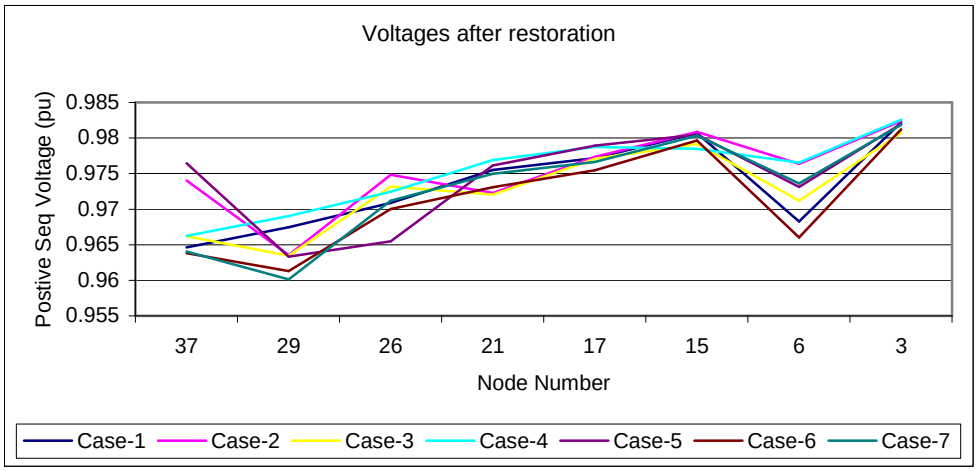

Figure 4.12: Voltages after Restoration for Modified IEEE 37-Node System

The simulation results presented were obtained by using a 2GHz Pentium® 4 PC. The voltages and currents obtained for a particular switching scenario were verified using unbalanced power flow software. The accuracy of the results illustrate that this formulation is valuable for the restoration of unbalanced distribution systems.

4.7 Computational Complexity

The optimization problem is a difficult problem to solve due to its combinatorial nature. Table 4.11 contains a list of number of integers, linear and non-linear variables and constraints for the modified IEEE 13, 37-node systems and SPS. Since the integer variables for the 37-node test case depend on the location of the fault, the search space varies from a minimum of 6 to a maximum of 41 integer variables. The speed of solution of the problem depends on how well it is formulated.

Table 4.11: Size of Optimization Problem

Elements	Type	Modified IEEE 13 - Node	Modified IEEE 37 - Node	SPS
Variables	Integer	14	6-41	8
	Linear	85	529	41
	Non - Linear	282	482	24
Constraints	Linear	199	728	84
	Non - Linear	167	279	19

The software LINGO did not pose any problem for the restoration of SPS, due to less non-linearity. For the unbalanced systems, LINGO failed to converge even for a small 4-node system. The formulations were changed to magnitude and angle instead of real and imaginary. The solution resulted in angles shifted by 2π and the currents became negative. This outcome was not acceptable. Even after the 4-node IEEE test system converged, the larger IEEE 13-node system failed to converge. LINGO updated their software, and after that patch was installed, the system solution converged for IEEE 13-node system. LINGO is still working on a newer version of the software, which may be

better than the existing version and would solve combinatorial problems faster than it does at present.

4.8 Summary

This chapter formulates the restoration problem for both balanced SPS and unbalanced terrestrial distribution systems. The SPS have an IPS where the power system is both AC and DC. The formulation of unbalanced distribution systems is different from the SPS, as the SPS have some special characteristics that need to be incorporated. Also, the power flow equality constraints for SPS cannot be applied to unbalanced distribution systems, as they show poor convergence.

CHAPTER V

UNBALANCED POWER FLOW WITH MULTIPLE DGS AND THEIR IMPACT ON DISTRIBUTION SYSTEMS

5.1 Introduction

This chapter presents the steady state analysis of TDS and SPS. It also describes the system studies on an IEEE 37-node feeder. The power flow software developed here incorporates the distinctive features of SPS, i.e., tightly connected, ungrounded, delta-connected with multiple generators. The software incorporates grounded wye connections, also. Distribution systems normally operate radially; hence the software works on radial systems only at present. Incorporating a distributed generator model in the software helps combat the technical difficulties associated with the fast growth of distributed generators in the distribution system. Component models developed in [67] are presented in detail and power flow update equations for each model are given. The algorithm is based on the backward forward sweep method and utilizes voltages and currents instead of real and reactive power. The algorithm does not involve matrix inversion and hence is very fast. This speed can help in distribution automation applications. The algorithm converged even if the R/X ratio was considerably high. The software was developed in MATLAB. The solution from the software was tested with RDAP, and the results matched very well.

Then, distributed generators were incorporated in the system. However RDAP could not verify the results, because it does not have the facility to model DG. The convergence for the DG occurs outside of the power flow, i.e., after the power flow has converged. This chapter also highlights the inputs needed by the software and a sample of the output.

5.2 Description of the Algorithm

First, the data is read and then the buses are renumbered by the algorithm. The algorithm proceeds from the end node to the top node, so this renumbering ensures that currents of all laterals are known before calculating currents for the node. Figure 5.1 shows the flow chart of the algorithm. After the algorithm renumbers the nodes, the power flow is run, and if it converges and some DGs are modeled as PV nodes, then the algorithm calculates the current to be injected by the DG and the power flow runs again.

5.2.1 Node Renumbering

The number of equations and unknowns in this algorithm depend not on the number of nodes but on the number of laterals. Proper node numbering reduces the number of equations and variables. A radial system can be thought of as a main feeder with laterals. These laterals may also have sub-laterals, which may have sub-laterals, etc. This renumbering is done in a depth-first order as shown in Figure 5.2, numbering the node and then all its laterals before numbering another node.

5.2.2 Method Description

This method involves two sweeps of calculations. In the forward sweep the end voltages are initialized for the first iteration and currents are calculated starting at the

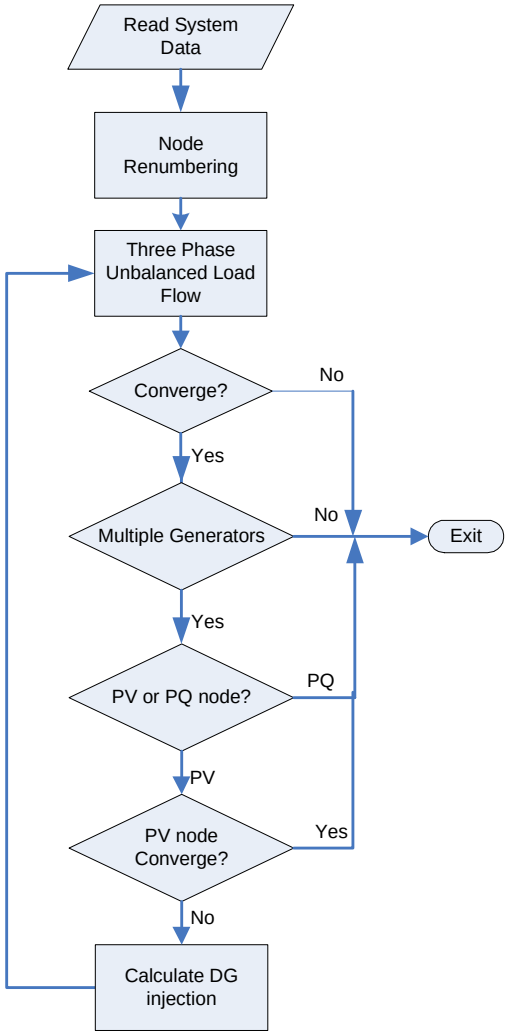

Figure 5.1: Flow Chart of the Power Flow Algorithm

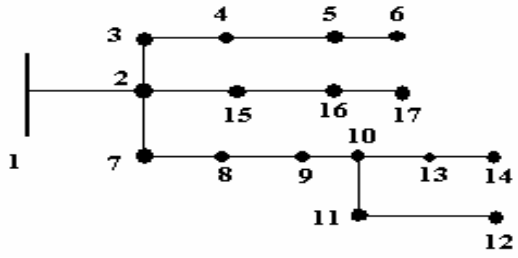

Figure 5.2: Node Renumbering

endmost buses and solved up to the source bus by applying the current summation method. Figure 5.3 shows the trace of the sweep by arrows. These currents are stored and used in the backward sweep calculations. The calculated source voltage (V_c) is compared with the specified voltage at the source node (V_s) to determine if it satisfies the termination criterion.

$$\delta V = \max_{i \in ph} | V_S^i - V_C^i | \leq \varepsilon \tag{5.1}$$

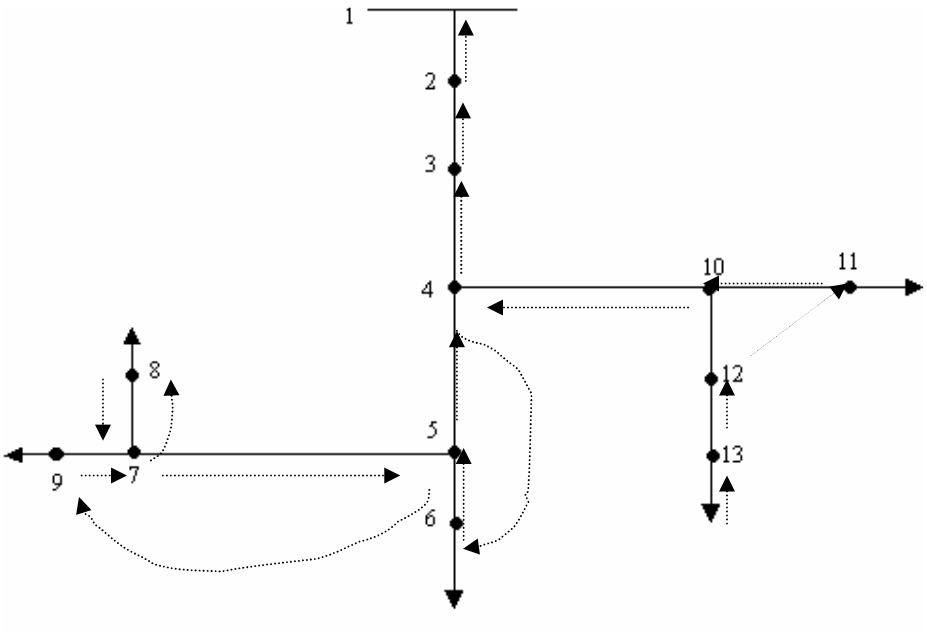

Figure 5.3: Forward Sweep Trace

The backward sweep starts at the source bus using the specified voltage and solves the network to the endmost buses calculating voltages using the currents calculated from the forward sweep. The voltages from the backward sweep are used for the next iteration in the forward sweep calculations.

5.3 Component Models

In any problem where numerical algorithms analyze a physical system, the results highly depend on the accuracy of mathematical models used. The power flow analysis models each component of the system as accurately as possible. Models which are too detailed become unusable due to unavailability of parameter data. Components can be categorized as in-branch components and node components. The first three components described in this section belong to the former category and the rest of the components belong to the latter category. For the in-branch components, whether the system is delta or wye connected, the line-neutral voltage and line currents are used for the update equation. For the node components, the line-to-line voltage and phase currents are used for a delta connected system, and line to neutral voltage and line currents are used for the wye connected system. So the component currents are transferred from phase currents to line currents in the software, before the update equations are applied.

5.3.1 Distribution System Line Model

The algorithm calculates the impedance of overhead lines and underground cables. Tables 2 and 3 in [68] help calculate the impedance of overhead lines from the given phasing, space ID, material and stranding. Tables 4, 5 and 6 in the same reference help calculate the impedance of underground concentric or tape shield cables. The developed impedance matrices model the lines. The phase admittance matrix does not have a significant contribution, and hence it is neglected.

Forward Sweep

$$V_i = V_{i+1} + ZI_{i+1} \tag{5.2}$$

$$I_i = I_{i+1}$$

Backward Sweep

$$V_i^{new} = V_{spec} - ZI_i \quad \text{for the first node calculation} \tag{5.3}$$

$$V_{i+1} = V_i^{new} - ZI_{i+1}$$

where,

i is the node number

V_i is the 3×1 complex vector of voltages for phases a, b and c

Z is the 3×3 mutually coupled impedance matrix

I_i is the 3×1 complex vector of currents for phases a, b and c

5.3.2 Three-Phase Transformer Model

Transformers are modeled as in [69] and only the update equations are given here. Four different types of transformers have been modeled, delta-wye, wye-delta, wye-wye and delta-delta.

Forward Sweep

$$V_i = a_t V_{i+1} + b_t I_{i+1} \tag{5.4}$$

$$I_i = d_t I_{i+1}$$

Backward Sweep

$$V_{i+1} = A_t V_i^{new} - B_t I_{i+1} \tag{5.5}$$

where a_t, b_t, c_t, d_t, A_t and B_t are the 3×3 matrices whose elements depend on the type of transformer.

5.3.3 Switch Model

Switches are modeled as branches with zero impedance

Forward Sweep

$$V_i = K * V_{i+1} \tag{5.6}$$

$$I_i = K * I_{i+1}$$

Backward Sweep

$$V_i^{new} = K * V_{spec} \tag{5.7}$$

$$V_{i+1} = K * V_i^{new}$$

where,

K (0/1) is the switch status.

5.3.4 Capacitor Model

The capacitor is modeled as a constant impedance matrix. The impedance is calculated once using the nominal voltage and nominal apparent power. This impedance is kept constant through out the power flow calculations. The current injection into node *i* changes as the voltage does, as seen from Equation (5.8 a and 5.8b).

$$Z_i^{ph-n} = \frac{\left|V_i^{ph-n}\right|^2}{S_i^{ph-n^*}}, IC_i^{ph-n} = \frac{V_i^{ph-n}}{Z_i^{ph-n}}, \text{ if the capacitor bank is wye connected} \tag{5.8a}$$

$$Z_i^{ph-ph} = \frac{\left|V_i^{ph-ph}\right|^2}{S_i^{ph-ph^*}}, IC_i^{ph-ph} = \frac{V_i^{ph-ph}}{Z_i^{ph-ph}}, \text{ if the capacitor bank is delta connected (5.8b)}$$

5.3.5 Load Model

One-, two- or three-phase loads with wye or delta connection can exist. Also, the loads fit into three different categories, depending on their characteristics. This section gives a brief description of the load model; Table 5.1 contains the models.

Constant Power: Real and reactive power injections at the bus are kept constant at the specified nominal values. This load corresponds to the traditional PQ approximation in transmission system analysis. But it is defined between any two nodes and not from node-to-ground as in traditional techniques.

Table 5.1: Load Models

Load Type	Model Equation	
	Wye	Delta
Const PQ	$IL_i^{ph} = \left(\frac{S_i^{ph-n}}{V_i^{ph-n}}\right)^*$	$IL_i^{ph} = \left(\frac{S_i^{ph-ph}}{V_i^{ph-ph}}\right)^*$
Const Z	$Z_i^{ph-n} = \frac{\left\|V_i^{ph-n}\right\|^2}{S_i^{ph-n^*}}$, $IL_i^{ph-n} = \frac{V_i^{ph-n}}{Z_i^{ph-n}}$	$Z_i^{ph-ph} = \frac{\left\|V_i^{ph-ph}\right\|^2}{S_i^{ph-ph^*}}$, $IL_i^{ph-ph} = \frac{V_i^{ph-ph}}{Z_i^{ph-ph}}$
Const I	$IL_i^{ph-n} = \left\|IL_i^{ph-n}\right\| * \angle\delta_i^{ph-n} - \theta_i^{ph-n}$	$IL_i^{ph-ph} = \left\|IL_i^{ph-ph}\right\| * \angle\delta_i^{ph-ph} - \theta_i^{ph-ph}$

Constant Impedance: These types of loads are useful to model large industrial

loads. The impedance of the load is calculated by the specified real and reactive power at nominal voltage and is kept constant throughout the power flow calculations.

Constant Current: The magnitude of the load current is calculated by the specified real and reactive power at nominal voltage and is kept constant. The angle of the current changes, depending on the voltage angle and the nominal power angle.

5.3.6 Distributed Load Model

Sometimes the primary feeder supplies loads through distribution transformers at various locations along line section. If a node is assumed at every load connection, then the system will have a large number of nodes. Therefore, these loads are represented as unified loads by lumping them:

1. At one-fourth length of line from the sending node where two thirds of the load is connected. For this a dummy node is created.
2. One-third load is connected at the receiving node.

Table 5.2 tabulates the summaries of the modeling equations for various components of the distribution system.

5.3.7 DG Model

Transmission power flow programs model generator buses by specifying voltage-angle (slack), real power-voltage (PV) or real-reactive power (PQ).For three-phase analysis, merely extending these constraints to each phase of a generator bus may lead to incorrect results. The generator connections can be wye or delta. Depending on its excitation and governor control, a DG may be set to output power at either constant pow-

Table 5.2: Component Models

<table>
<tr><th>Component</th><th colspan="2">Backward Sweep</th><th>Forward Sweep</th></tr>
<tr><td>Overhead Lines/Under-ground Cables</td><td colspan="2">$V_i^{new} = V_{spec} - ZI_i$ for the first node calculation
$V_{i+1} = V_i^{new} - ZI_{i+1}$</td><td>$V_i = V_{i+1} + ZI_{i+1}$
$I_i = I_{i+1}$</td></tr>
<tr><td>Three-phase Transformer</td><td colspan="2">$V_{i+1} = A_t V_i^{new} - B_t I_{i+1}$</td><td>$V_i = a_t V_{i+1} + b_t I_{i+1}$
$I_i = d_t I_{i+1}$</td></tr>
<tr><td>Switch</td><td colspan="2">$V_i^{new} = K * V_{spec}$
$V_{i+1} = K * V_i^{new}$</td><td>$V_i = K * V_{i+1}$
$I_i = K * I_{i+1}$</td></tr>
<tr><td>Capacitor</td><td colspan="3">$Z_i^{ph-n} = \frac{\left|V_i^{ph-n}\right|^2}{S_i^{ph-n^*}}, IC_i^{ph-n} = \frac{V_i^{ph-n}}{Z_i^{ph-n}}$ Wye Connected
$Z_i^{ph-ph} = \frac{\left|V_i^{ph-ph}\right|^2}{S_i^{ph-ph^*}}, IC_i^{ph-ph} = \frac{V_i^{ph-ph}}{Z_i^{ph-ph}}$ Delta Connected</td></tr>
<tr><td rowspan="4">Load</td><td>Load Type</td><td>Wye</td><td>Delta</td></tr>
<tr><td>Const PQ</td><td>$IL_i^{ph} = \left(\frac{S_i^{ph-n}}{V_i^{ph-n}}\right)^*$</td><td>$IL_i^{ph} = \left(\frac{S_i^{ph-ph}}{V_i^{ph-ph}}\right)^*$</td></tr>
<tr><td>Const Z</td><td>$Z_i^{ph-n} = \frac{\left|V_i^{ph-n}\right|^2}{S_i^{ph-n^*}}$,
$IL_i^{ph-n} = \frac{V_i^{ph-n}}{Z_i^{ph-n}}$</td><td>$Z_i^{ph-ph} = \frac{\left|V_i^{ph-ph}\right|^2}{S_i^{ph-ph^*}}$,
$IL_i^{ph-ph} = \frac{V_i^{ph-ph}}{Z_i^{ph-ph}}$</td></tr>
<tr><td>Const I</td><td>$IL_i^{ph-n} = \left|IL_i^{ph-n}\right| *$
$\angle\delta_i^{ph-n} - \theta_i^{ph-n}$</td><td>$Z_i^{ph-ph} = \frac{\left|V_i^{ph-ph}\right|^2}{S_i^{ph-ph^*}}$,
$IC_i^{ph-ph} = \frac{V_i^{ph-ph}}{Z_i^{ph-ph}}$</td></tr>
<tr><td>Distributed Load</td><td colspan="3">1. Two thirds load is lumped at one-fourth length of line from sending node.
2. One-third load is lumped at the receiving node.</td></tr>
</table>

-er factor for a limited reactive power DG or a small DG, or constant voltage for a large DG. In other words, some DGs are modeled as constant PQ negative loads with currents injecting into the node, and others are modeled as PV nodes. The PV node modeling of DG needs a special form of analysis to be incorporated in the radial power flow program. The power flow solution determines the node voltages and the terminal voltage of the generator, which determines the amount of current injection from the generator when modeled as a PV node. A DG in this mode behaves as a voltage-dependent current source. Since the terminal voltages are unbalanced, the injected currents will also be unbalanced as shown in Figure 5.4. A large imbalance in currents is detrimental for the generator operation, and hence the generator will shut down. A generator terminal voltage is typically controlled by the specification of a positive sequence component. Thus, the injected power of each phase, under an unbalanced terminal voltage condition, can be calculated. Steps for incorporating the PV node are as follows:

Initially, the generator real power and positive sequence voltage is specified. The reactive power is initialized to zero. After a power flow has converged, it is checked to determine if the voltage magnitude mismatch at the PV node is below a specified tolerance.

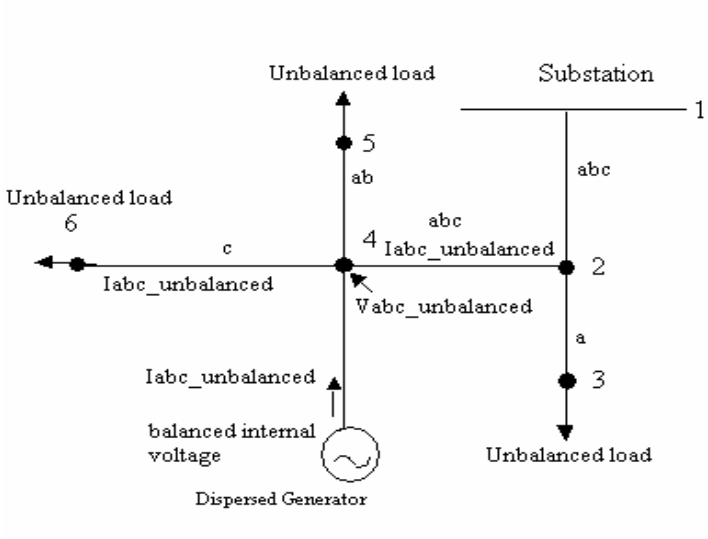

Figure 5.4: Effect of Unbalance of the System on DG Injection

1. The specified voltage is a positive sequence terminal voltage of the PV node.

$$\Delta V_1^{\,j} = \left|V_{1sp}^{\,j}\right| - \left|V_{1cal}^{\,j}\right| \le \varepsilon \tag{5.9}$$

where $j \in$ set S of PV nodes.

2. If the voltage mismatch is within the specified tolerance, the PV node voltage has converged to the specified value. If a voltage mismatch at the PV node is not less than the specified tolerance, then the reactive power compensation Q generated by that PV node in order to maintain the voltage at specified value needs to be calculated.

$$Z_{1pv} * \Delta I_q = \Delta V_{1pv} \tag{5.10}$$

where Z_{1PV} is the sequence sensitivity impedance matrix, whose size is $n_{pv} \times n_{pv}$. The diagonal elements of this matrix are the absolute value of the positive sequence of sum of series line impedances between each PV node and the source node. The off diagonal

elements are calculated from the shared path between two PV nodes and source node. ΔV_{1pv} is $n_{pv} \times 1$. Thus ΔI_q is $n_{pv} \times 1$ and is the magnitude of reactive current injection.

3. The reactive current injection is then

$$\begin{aligned} \Delta I_{qa}^{j} &= \Delta I_{q}^{j} * e^{j(\mathrm{sgn}(\Delta V_1^j)*90^\circ + \delta v_a^j)} \\ \Delta I_{qb}^{j} &= \Delta I_{q}^{j} * e^{j(\mathrm{sgn}(\Delta V_1^j)*90^\circ + \delta v_b^j)} \\ \Delta I_{qc}^{j} &= \Delta I_{q}^{j} * e^{j(\mathrm{sgn}(\Delta V_1^j)*90^\circ + \delta v_c^j)} \end{aligned} \tag{5.11}$$

where, $\delta V_a^j, \delta V_b^j$ and δV_c^j are the angles of the converged voltage at the jth PV node; the *sgn* is used so that the reactive power can be absorbed or injected. This current and the converged voltage are used to calculate the reactive current being injected or absorbed.

4. Now these currents are added to the currents calculated in previous iterations at the jth node. If any previously injected reactive power exists, it is added to the presently calculated reactive power and checked to determine if the total reactive power that the generator is producing is within the limits.

$$\begin{aligned} I_{qa}^{j} &= I_{qa}^{j} + \Delta I_{qa}^{j} \\ I_{qb}^{j} &= I_{qb}^{j} + \Delta I_{qb}^{j} \\ I_{qc}^{j} &= I_{qc}^{j} + \Delta I_{qc}^{j} \end{aligned} \tag{5.12}$$

There is a limit to which the DG can produce reactive power; and this limit is decided in this program by setting the power factor limits between 0.8 and 1 lagging/leading. If during the computation, the reactive power of any of the DGs exceeds its limits, it is fixed at the limiting value and this node is now treated as PQ node.

$$Q_{G,\min}^{j} \le Q_{G}^{j} \le Q_{G,\max}^{j} \tag{5.13}$$

The limiting value is calculated as the three-phase reactive power limit; thus, the total per phase reactive current that the DG can inject before its limit is hit is given by:

$$\Delta I^{j}_{q,\lim it} = \frac{\frac{Q^{j}_{G,\lim it}}{3}}{mag(V^{j}_{1})} \tag{5.14}$$

The power flow runs again to check the voltage magnitudes and new ΔV^{j}_{1}. If in the next iteration the Q_G of the PV node converted to PQ node is within the limits the node is switched back to PV node. With multiple distributed generators, a check is made to see which DGs hit the limit, and they inject the limiting current. However, if all DGs hit limits, and the voltage is not at its specified value, the algorithm terminates and prints that the DGs have hit limits and real power needs to be increased. The solution algorithm is summarized in the flow chart given in Figure 5.5.

5.4 Steps for Performing Unbalanced Power Flow

Distribution systems consist of a main feeder, laterals and sublaterals. Consider the feeder in Figure 5.3. First, the feeder is renumbered, and then the following steps are performed:

1. Assume three-phase L-N voltages at all the end nodes (6, 8, 9, 11 and 13). Start at the higher most numbered end node (13).
2. Calculate load currents if any at node 13 using the load component equations in Table 5.2. If the load is delta connected, the currents are later converted to line currents. These load currents are also the currents in the overhead lines.

3. Calculate the voltage and current of node 12 using the overhead line model in Table 5.2. Similarly, calculate the voltage and current at node 10.
4. Then the junction node 10 is encountered. Calculations are not made for this node unless all downstream nodes from this node are calculated. So the load currents for node 11 are calculated and then voltage and current for node 10 are calculated in a similar manner to steps 2 and 3 above.
5. The most recent voltage for node 10 is considered and the voltage for node 4 is calculated. The current for node 10 is the summation of currents obtained from node 12 and 11 as well as load currents if any at node 10. Similar to node 10, calculations are not made for node 4, unless calculations of all downstream nodes to node 4 are completed.
6. Load currents for node 6 are calculated. If there had been a transformer between nodes 5 and 6, then the transformer component equations from Table 5.2 would have been utilized. But, since there is no transformer, the line component equations are utilized to calculate the voltages at node 5.
7. Since node 9 is a single-phase node only the “c” phase current is calculated and only the “c” phase current and voltage of node 7 is obtained from node 9. Since node 8 is a single-phase node only the “a” phase current is calculated and only the “a” phase current and voltage of node 7 is obtained from node 8.
8. Since node 7 is two-phase node the voltages calculated from node 9 and node 8 both are considered and the most recent voltage criterion is discarded.
9. Node 5 voltage is calculated and since node 5 is three-phase node the voltages for

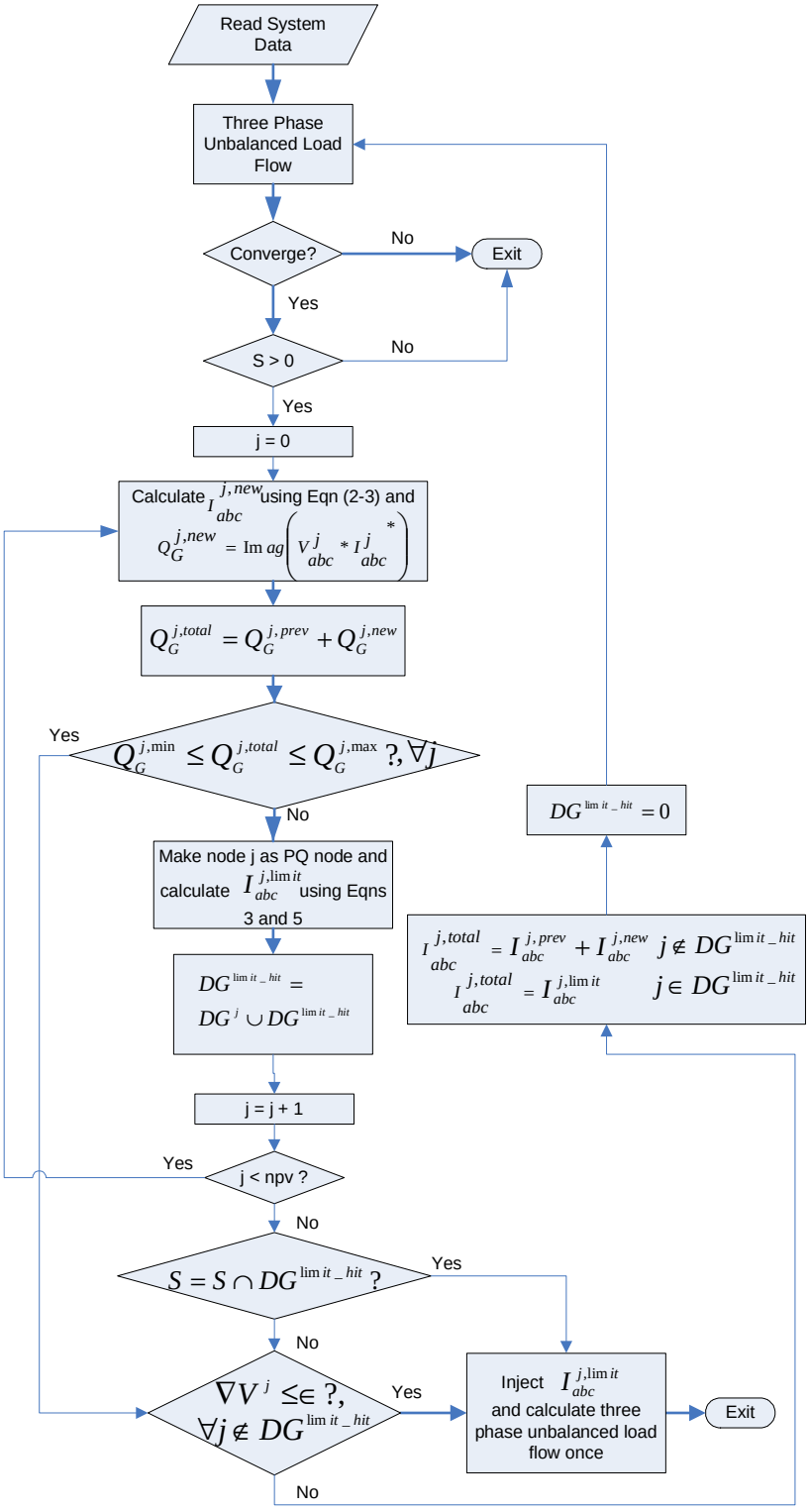

Figure 5.5: Flow Chart for Power Flow with Multiple DGs

"a" and "c" phases are the most recent voltages calculated from node 7 however the b phase voltage is that calculated from node 6.

10. Voltages are calculated for nodes 4, 3, 2 and 1. Equation 5.1 is used to calculate the error and if the error is not within tolerance the backward sweep progresses.
11. Using the currents calculated in the forward sweep, voltages are calculated using the appropriate component equations. The calculations proceed in exactly the opposite order of the forward sweep calculations.
12. The sweeps continue until the first node voltage is within the tolerance. If it is in tolerance, then the power flow is said to have converged.
13. At this stage, it is checked if there are any DGs in the system. If there are DGs and if the DG is a PQ node, it has been already taken care of while calculating the load current, as a PQ node model is treated as a negative load. If the DG is a PV model, then steps 1-3 in Section 5.3.7 are followed. The power flow is run again and the voltage at the DG node is checked. If the voltage is within the tolerance the program stops and prints the results
14. If the voltage is outside the tolerance limit, then the current to be injected to correct the voltage further is calculated. This current in then added to the previously injected current and the power flow analysis is run again.

5.5 Description of Test Systems

The IEEE 13-node and 37-node systems described in Chapter 4 were considered. The regulator was removed from both the systems to clearly see the effect of the DG on the system, with no other assumptions or modifications. Apart from these two systems, an

18-node SPS of the Healy icebreaker ship was also analyzed, for which the data was obtained from [55]. Figure 5.6 shows the layout of the Healy system. Figure 5.7 depicts the system's representation with renumbering, so that the analysis could be done using the developed unbalanced power flow software. The data is characterized by

- Loads – Spot loads, three-phase balanced loads, delta connected, constant kW, kVAR.
- Overhead and Underground Lines – Three-phase cables.
- Transformer – Inline transformer is delta-delta with tap ratio one.

5.6 Unbalanced Power Flow Results

The IEEE PES Distribution System subcommittee has obtained the power flow analysis of the radial IEEE distribution feeders using RDAP.

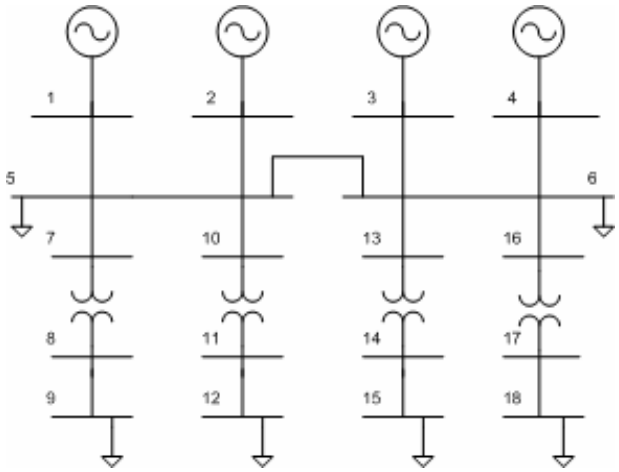

Figure 5.6: Healy Icebreaker Ship System

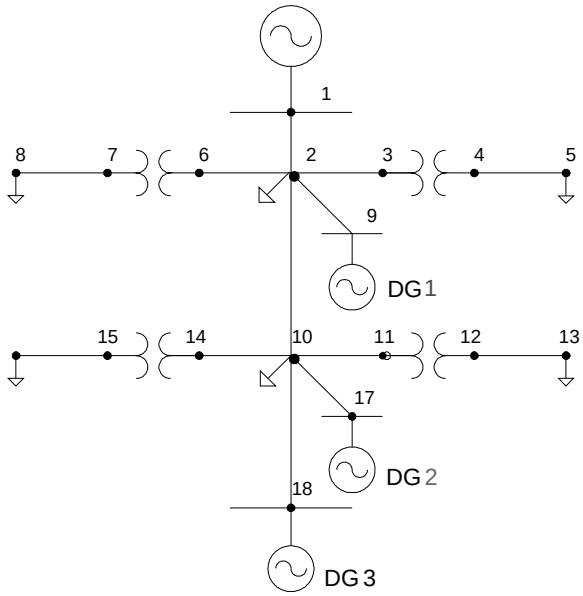

Figure 5.7: Renumbered Shipboard Power System

5.6.1 IEEE 13-Node System

The feeder was analyzed without DG, with DG modeled as a PQ node and with DG modeled as a PV node.

A. Original Feeder Analysis

The comparison of the results of the original feeder (without DG) obtained by the developed program and those obtained by RDAP are shown in Tables 5.3 and 5.4. As seen from the Tables the results obtained from the developed program closely match the results obtained from RDAP. The power flow took three iterations to converge. However, voltage violations occur at many nodes though the desirable voltage is in the range of 0.95 and 1.05 pu.

Table 5.3: Original Feeder Analysis (Voltages)

Node ID	Calculated		RDAP		Calculated		RDAP		Calculated		RDAP	
	Van	∠Van	Van	∠Van	Vbn	∠Vbn	Vbn	∠Vbn	Vcn	∠Vcn	Vcn	∠Vcn
650	1	0	1	0	1	-120	1	-120	1	120	1	120
632	0.9566	-2.75	0.9559	-2.79	0.9907	-121.85	0.9909	-121.83	0.9443	117.61	0.9441	117.6
645					0.9811	-122.05	0.9815	-122.01	0.9424	117.64	0.9424	117.62
646					0.9793	-122.13	0.9799	-122.09	0.9403	117.69	0.9405	117.67
633	0.9533	-2.82	0.9528	-2.86	0.9887	-121.91	0.9889	-121.88	0.9417	117.62	0.9413	117.6
634	0.9277	-3.59	0.9271	-3.64	0.9694	-122.41	0.9696	-122.38	0.9214	117.067	0.921	117.04
671	0.9237	-5.89	0.9232	-5.95	1.0011	-122.52	1.0015	-122.49	0.9009	115.61	0.9003	115.58
692	0.924	-5.88	0.9232	-5.95	1.0011	-122.52	1.0015	-122.49	0.9009	115.61	0.9003	115.58
675	0.9168	-6.16	0.9161	-6.22	1.0035	-122.71	1.0039	-122.68	0.8986	115.64	0.898	115.61
684	0.9219	-5.91	0.9214	-5.97					0.8988	115.50	0.8981	115.47
611									0.8967	115.35	0.896	115.32
652	0.916	-5.83	0.9154	-5.9								
680	0.9238	-5.88	0.9232	-5.95	1.0011	-122.52	1.0015	-122.49	0.9009	115.61	0.9003	115.58

Table 5.4: Original Feeder Analysis (Currents)

From – To Node	Calculated		RDAP		Calculated		RDAP		Calculated		RDAP	
	|Ia|	∠Ia	|Ia|	∠Ia	|Ib|	∠Ib	|Ib|	∠Ib	|Ic|	∠Ic	|Ic|	∠Ic
650-632	591.76	-29.63	592.02	-29.68	440.44	-142.51	435.62	-142.72	626.22	91.75	622.39	91.98
632-633	87.14	-38.1	87.2	-38.14	64.43	-159.28	64.41	-159.25	67.78	80.2	67.81	80.17
632-645					148.59	-143.3	143.83	-143.97	66.35	57.26	61.29	57.26
632-671	505.72	-28.18	505.94	-28.23	231.1	-137.39	231.07	-137.39	507.71	97.53	507.98	97.49
645-646					61.25	-122.74	61.29	-122.74	61.25	57.26	61.29	57.26
633-634	755.25	-38.1	755.73	-38.15	558.37	-159.28	558.22	-159.25	587.45	80.2	587.7	80.17
671-692	246.55	-20.57	246.76	-20.65	65.1	-58.39	65.16	-58.33	191.02	105.16	191.14	105.1
671-684	58.81	-39.73	58.76	-39.77					70.9	118.61	70.89	118.56
671-680	0	0	0	0	0	0	0	0	0	0	0	0
692-675	220.49	-8.74	220.67	-8.84	65.1	-58.39	65.16	-58.33	136.39	105.77	136.5	105.7
684-611									70.9	118.61	70.89	118.55
684-652	58.81	-39.73	58.76	-39.77								

B. DG as PQ Node

A delta-connected DG was introduced on node 671 and the node was treated as a PQ node with constant power factor of 0.9. The capacity of the installed DG was 1.89

MW and 0.915 MVAR, which is 55% of the total three-phase load in the system. The power flow converged in three iterations. As seen from Tables 5.5 and 5.6, the results obtained from the developed program closely match the results obtained from RDAP when the DG node is modeled as a PQ node.

Table 5.5: Feeder Analysis with PQ Node (Voltages)

Node ID	Calculated		RDAP		Calculated		RDAP		Calculated		RDAP	
	Van	∠Van	Van	∠Van	Vbn	∠Vbn	Vbn	∠Vbn	Vcn	∠Vcn	Vcn	∠Vcn
650	1	0	1	0	1	-120	1	-120	1	120	1	120
632	0.9817	-1.66	0.9815	-1.68	1.008	-120.48	1.0081	-120.47	0.9707	118.84	0.9707	118.84
645					0.9986	-120.67	0.9988	-120.65	0.9688	118.86	0.969	118.86
646					0.9968	-120.74	0.9971	-120.72	0.9668	118.91	0.967	118.91
633	0.9785	-1.73	0.9784	-1.75	1.006	-120.53	1.0062	-120.52	0.968	118.83	0.968	118.83
634	0.9536	-2.47	0.9534	-2.48	0.987	-121.02	0.9872	-121	0.9483	118.31	0.9483	118.31
671	0.9725	-3.53	0.9725	-3.55	1.035	-119.81	1.0351	-119.8	0.9522	118.21	0.9522	118.21
692	0.9727	-3.53	0.9725	-3.55	1.035	-119.81	1.0351	-119.8	0.9522	118.21	0.9522	118.21
675	0.966	-3.78	0.9659	-3.8	1.0374	-119.99	1.0375	-119.98	0.9501	118.23	0.9501	118.23
684	0.9707	-3.55	0.9706	-3.57					0.9501	118.11	0.9501	118.11
611									0.9481	117.96	0.9481	117.96
652	0.9645	-3.48	0.9644	-3.5								
680	0.9726	-3.53	0.9725	-3.54	1.035	-119.81	1.0351	-119.8	0.9522	118.21	0.9522	118.21

Table 5.6: Feeder Analysis with PQ Node (Currents)

From – To Node	Calculated		RDAP		Calculated		RDAP		Calculated		RDAP	
	|Ia|	∠Ia	|Ia|	∠Ia	|Ib|	∠Ib	|Ib|	∠Ib	|Ic|	∠Ic	|Ic|	∠Ic
650-632	273.95	-26.45	273.97	-26.45	137.03	-123.18	134.94	-123.15	304.15	97.39	302.55	97.63
632-633	84.78	-36.98	84.79	-36.99	63.28	-157.89	63.26	-157.87	65.86	81.44	65.86	81.44
632-645					145.6	-141.93	143.63	-142.21	64.81	58.73	62.72	58.74
632-671	191.23	-21.8	191.24	-21.8	98.26	-0.64	98.31	-0.65	199.04	114.51	199.05	114.49
645-646					62.71	-121.27	62.72	-121.26	62.81	58.73	62.72	58.74
633-634	734.75	-36.98	734.86	-36.99	548.4	-157.89	548.29	-157.87	570.77	81.44	570.78	81.44
671-692	233.67	-16.86	233.69	-16.88	68.02	-53.65	68.05	-53.62	182.28	110.25	182.27	110.26
671-684	61.92	-37.38	61.9	-37.36					71.05	122.94	71.05	122.94
671-680	0	0	0	0	0	0	0	0	0	0	0	0
692-675	209.05	-4.19	209.07	-4.2	68.02	-53.65	68.05	-53.62	127.83	112.04	127.82	112.05
684-611									71.05	122.94	71.05	122.94
684-652	61.92	-37.38	61.9	-37.36								

C. DG as PV Node

A delta-connected DG of the same capacity as the PQ node model above was introduced on node 671. The DG node was then modeled as PV node. The specified positive sequence voltage at this node was 1.0 pu. The total three-phase Q injected in this case was 1.437 MVAR. The power flow converged in three iterations after the injection. RDAP does not have the facility to model DG as a PV node. Tables 5.7 and 5.8 show the results obtained. The positive sequence voltage at node 671 is maintained at 1.00 pu. Also, due to the DG, the node voltages at all other nodes have improved. A snapshot of the output from the developed software is as shown in Figure 5.8.

5.6.2 IEEE 37-Node System

In this section the feeder is analyzed without DG. Section 5.7 presents the results of the study on this system with DG.

Table 5.7: Feeder Analysis with PV Node (Voltages)

Node ID	Van	∠Van	Vbn	∠Vbn	Vcn	∠Vcn
650	1	0	1	-120	1	120
632	0.9888	-1.81	1.0136	-120.55	0.9789	118.74
645			1.0043	-120.73	0.977	118.77
646			1.0025	-120.81	0.975	118.81
633	0.9857	-1.88	1.0116	-120.60	0.9762	118.74
634	0.9609	-2.60	0.9928	-121.08	0.9566	118.22
671	0.9872	-3.79	1.046	-119.96	0.9685	118.02
692	0.9872	-3.79	1.046	-119.96	0.9685	118.02
675	0.9807	-4.05	1.0484	-120.14	0.9666	118.04
684	0.9852	-3.82			0.9665	117.92
611					0.9645	117.77
652	0.9789	-3.75				
680	0.9872	-3.80	1.046	-119.96	0.9685	118.02

Table 5.8: Feeder Analysis with PV Node (Currents)

From-To Node	|Ia|	∠Ia	|Ib|	∠Ib	|Ic|	∠Ic
650-632	249.34	-9.22	153.99	-98.08	273.22	111.51
632-633	84.13	-37.11	62.91	-157.96	65.29	81.35
632-645			144.68	-142	64.35	58.69
632-671	179.35	3.46	155.83	-14.79	196.75	136.8
645-646			62.35	-121.31	62.35	58.69
633-634	729.11	-37.11	545.2	-157.96	565.8	81.35
671-692	230.06	-16.71	68.98	-53.19	179.74	110.87
671-684	62.85	-37.64			71.11	123.3
671-680	0	0	0	0	0	0
692-675	205.91	-3.77	68.98	-53.19	125.4	113.08
684-611					71.11	123.3
684-652	62.85	-37.64				

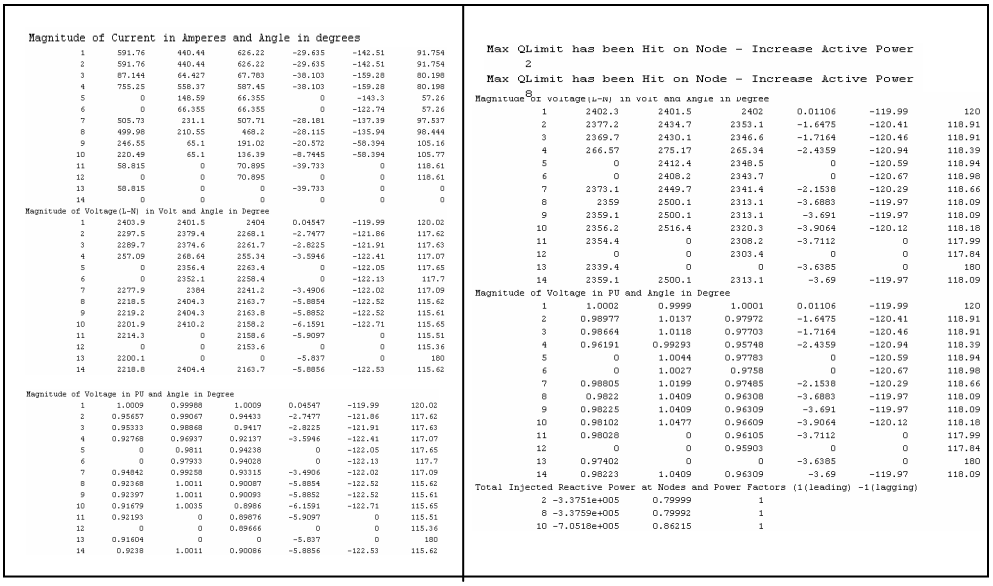

Magnitude of Current in Amperes and Angle in degrees

1	591.76	440.44	626.22	-29.635	-142.51	91.754
2	591.76	440.44	626.22	-29.635	-142.51	91.754
3	87.144	64.427	67.703	-38.103	-159.28	80.198
4	755.25	558.37	587.45	-38.103	-159.28	80.198
5	0	148.59	66.355	0	-143.3	57.26
6	0	66.355	66.355	0	-122.74	57.26
7	505.73	231.1	507.71	-28.181	-137.39	97.537
8	499.98	210.55	468.2	-28.115	-135.94	98.444
9	246.55	65.1	191.02	-20.572	-58.394	105.16
10	220.49	65.1	136.39	-8.7445	-58.394	105.77
11	58.815	0	70.895	-39.733	0	118.61
12	0	0	70.895	0	0	118.61
13	58.815	0	0	-39.733	0	0
14	0	0	0	0	0	0

Magnitude of Voltage(L-N) in Volt and Angle in Degree

1	2403.9	2401.5	2404	0.04547	-119.99	120.02
2	2297.5	2379.4	2268.1	-2.7477	-121.86	117.62
3	2289.7	2374.6	2261.7	-2.8225	-121.91	117.63
4	257.09	268.64	255.34	-3.5946	-122.41	117.07
5	0	2356.4	2263.4	0	-122.05	117.65
6	0	2352.1	2258.4	0	-122.13	117.7
7	2277.9	2384	2241.2	-3.4906	-122.02	117.09
8	2218.5	2404.3	2163.7	-5.8854	-122.52	115.62
9	2219.2	2404.3	2163.8	-5.8852	-122.52	115.61
10	2201.9	2410.2	2158.2	-6.1591	-122.71	115.65
11	2214.3	0	2158.6	-5.9097	0	115.51
12	0	0	2153.6	0	0	115.36
13	2200.1	0	0	-5.837	0	180
14	2218.8	2404.4	2163.7	-5.8856	-122.53	115.62

Magnitude of Voltage in PU and Angle in Degree

1	1.0009	0.99988	1.0009	0.04547	-119.99	120.02
2	0.95657	0.99067	0.94433	-2.7477	-121.86	117.62
3	0.95333	0.98868	0.9417	-2.8225	-121.91	117.63
4	0.92768	0.96937	0.92137	-3.5946	-122.41	117.07
5	0	0.9811	0.94238	0	-122.05	117.65
6	0	0.97933	0.94028	0	-122.13	117.7
7	0.94842	0.99258	0.93315	-3.4906	-122.02	117.09
8	0.92368	1.0011	0.90087	-5.8854	-122.52	115.62
9	0.92397	1.0011	0.90093	-5.8852	-122.52	115.61
10	0.91679	1.0035	0.8986	-6.1591	-122.71	115.65
11	0.92193	0	0.89876	-5.9097	0	115.51
12	0	0	0.89666	0	0	115.36
13	0.91604	0	0	-5.837	0	180
14	0.9238	1.0011	0.90086	-5.8856	-122.53	115.62

Max QLimit has been Hit on Node - Increase Active Power
2
Max QLimit has been Hit on Node - Increase Active Power
8
Magnitude of Voltage(L-N) in Volt and Angle in Degree

1	2402.3	2401.5	2402	0.01106	-119.99	120
2	2377.2	2434.7	2353.1	-1.6475	-120.41	118.91
3	2369.7	2430.1	2346.6	-1.7164	-120.46	118.91
4	266.57	275.17	265.34	-2.4359	-120.94	118.39
5	0	2412.4	2348.5	0	-120.59	118.94
6	0	2408.2	2343.7	0	-120.67	118.98
7	2373.1	2449.7	2341.4	-2.1538	-120.29	118.66
8	2359	2500.1	2313.1	-3.6883	-119.97	118.09
9	2359.1	2500.1	2313.1	-3.691	-119.97	118.09
10	2356.2	2516.4	2320.3	-3.9064	-120.12	118.18
11	2354.4	0	2308.2	-3.7112	0	117.99
12	0	0	2303.4	0	0	117.84
13	2339.4	0	0	-3.6385	0	180
14	2359.1	2500.1	2313.1	-3.69	-119.97	118.09

Magnitude of Voltage in PU and Angle in Degree

1	1.0002	0.9999	1.0001	0.01106	-119.99	120
2	0.98977	1.0137	0.97972	-1.6475	-120.41	118.91
3	0.98664	1.0118	0.97703	-1.7164	-120.46	118.91
4	0.96191	0.99293	0.95748	-2.4359	-120.94	118.39
5	0	1.0044	0.97783	0	-120.59	118.94
6	0	1.0027	0.9758	0	-120.67	118.98
7	0.98805	1.0199	0.97485	-2.1538	-120.29	118.66
8	0.9822	1.0409	0.96308	-3.6883	-119.97	118.09
9	0.98225	1.0409	0.96309	-3.691	-119.97	118.09
10	0.98102	1.0477	0.96609	-3.9064	-120.12	118.18
11	0.98028	0	0.96105	-3.7112	0	117.99
12	0	0	0.95903	0	0	117.84
13	0.97402	0	0	-3.6385	0	180
14	0.98223	1.0409	0.96309	-3.69	-119.97	118.09

Total Injected Reactive Power at Nodes and Power Factors (1(leading) -1(lagging)

2	-3.3751e+005	0.79999	1
8	-3.3759e+005	0.79992	1
10	-7.0518e+005	0.86215	1

(a) (b)

Figure 5.8: Snapshot of the Output from the Developed Software (a) Without DG (b) With DG

A. Original Feeder Analysis

The results of the original feeder obtained by the developed program and those obtained by RDAP, as seen from Tables 5.9 and 5.10, closely match.

Table 5.9: Modified IEEE 37-Node Voltages

Node ID	Calculated		RDAP		Calculated		RDAP		Calculated		RDAP	
	Vab	∠Vab	Vab	∠Vab	Vbc	∠Vbc	Vbc	∠Vbc	Vca	∠Vca	Vca	∠Vca
799	1	0	1	0	1	-120	1	-120	1	120	1	120
701	0.989	-0.09	0.988	-0.08	0.99	-120.4	0.989	-120.41	0.985	119.69	0.984	119.69
702	0.982	-0.15	0.981	-0.14	0.984	-120.6	0.984	-120.61	0.976	119.49	0.976	119.49
713	0.98	-0.16	0.98	-0.15	0.982	-120.62	0.982	-120.63	0.974	119.5	0.974	119.5
704	0.978	-0.18	0.978	-0.18	0.98	-120.63	0.979	-120.64	0.972	119.52	0.972	119.52
720	0.977	-0.22	0.977	-0.22	0.977	-120.68	0.976	-120.69	0.97	119.59	0.969	119.6
707	0.976	-0.31	0.975	-0.31	0.971	-120.65	0.971	-120.66	0.968	119.74	0.968	119.74
724	0.975	-0.33	0.975	-0.33	0.97	-120.64	0.97	-120.65	0.968	119.76	0.967	119.77
722	0.975	-0.32	0.975	-0.32	0.971	-120.65	0.97	-120.65	0.968	119.75	0.967	119.76
706	0.977	-0.23	0.977	-0.22	0.976	-120.68	0.975	-120.69	0.97	119.6	0.969	119.6
725	0.977	-0.24	0.977	-0.23	0.976	-120.68	0.975	-120.69	0.97	119.61	0.969	119.61
714	0.978	-0.18	0.978	-0.18	0.98	-120.63	0.979	-120.63	0.972	119.52	0.972	119.52
718	0.977	-0.17	0.976	-0.16	0.98	-120.59	0.979	-120.6	0.972	119.49	0.971	119.48
705	0.981	-0.14	0.98	-0.13	0.983	-120.61	0.983	-120.62	0.975	119.52	0.974	119.52
742	0.981	-0.16	0.98	-0.15	0.982	-120.61	0.982	-120.61	0.975	119.54	0.974	119.54
712	0.981	-0.12	0.98	-0.11	0.983	-120.63	0.982	-120.64	0.974	119.53	0.974	119.52
703	0.975	-0.19	0.974	-0.18	0.981	-120.72	0.98	-120.73	0.97	119.24	0.969	119.24
727	0.974	-0.17	0.973	-0.16	0.98	-120.71	0.979	-120.72	0.969	119.24	0.968	119.23
744	0.973	-0.17	0.972	-0.16	0.979	-120.7	0.979	-120.71	0.968	119.22	0.967	119.21
729	0.972	-0.16	0.972	-0.15	0.979	-120.69	0.979	-120.7	0.968	119.21	0.967	119.21
728	0.972	-0.16	0.972	-0.15	0.979	-120.7	0.979	-120.71	0.968	119.22	0.967	119.22
730	0.97	-0.13	0.969	-0.12	0.978	-120.75	0.977	-120.76	0.964	119.15	0.963	119.14
709	0.968	-0.12	0.967	-0.11	0.977	-120.76	0.976	-120.77	0.963	119.11	0.962	119.11
775	0.968	-0.12	0.967	-0.1	0.977	-120.76	0.976	-120.77	0.963	119.11	0.962	119.1
731	0.968	-0.14	0.967	-0.12	0.976	-120.76	0.975	-120.77	0.963	119.14	0.962	119.13
708	0.965	-0.09	0.965	-0.08	0.976	-120.76	0.975	-120.77	0.961	119.05	0.96	119.04
732	0.965	-0.07	0.965	-0.06	0.976	-120.77	0.975	-120.78	0.96	119.05	0.959	119.04
733	0.963	-0.07	0.962	-0.05	0.975	-120.75	0.974	-120.76	0.959	118.99	0.958	118.98
734	0.96	-0.02	0.959	0	0.973	-120.76	0.973	-120.77	0.956	118.91	0.955	118.89
710	0.959	0.02	0.958	0.02	0.972	-120.79	0.972	-120.8	0.954	118.93	0.953	118.92
736	0.959	-0.03	0.958	-0.01	0.971	-120.77	0.97	-120.78	0.954	118.98	0.953	118.97
735	0.959	0.03	0.958	0.04	0.972	-120.8	0.971	-120.81	0.954	118.94	0.952	118.93
737	0.956	0.02	0.956	0.03	0.972	-120.73	0.972	-120.74	0.954	118.81	0.952	118.8
738	0.955	0.04	0.954	0.05	0.972	-120.73	0.971	-120.74	0.952	118.78	0.951	118.76
711	0.955	0.07	0.954	0.08	0.972	-120.76	0.971	-120.77	0.952	118.77	0.95	118.76
740	0.955	0.08	0.954	0.09	0.972	-120.77	0.971	-120.78	0.951	118.78	0.95	118.76
741	0.955	0.07	0.954	0.08	0.972	-120.77	0.971	-120.78	0.951	118.77	0.95	118.76

Table 5.10: Modified IEEE 37-Node Currents

From – To Node	Calculated		RDAP		Calculated		RDAP		Calculated		RDAP	
	|Ia|	∠Ia	|Ia|	∠Ia	|Ib|	∠Ib	|Ib|	∠Ib	|Ic|	∠Ic	|Ic|	∠Ic
799-701	373.58	-63.18	373.31	-63.09	276.66	-178.86	276.34	-178.72	355.72	72.318	355.63	72.44
701-702	271.54	-60.3	271.36	-60.2	219.49	-179.38	219.24	-179.26	252.92	70.379	252.82	70.51
702-713	59.973	-66.19	59.9	-66.08	71.81	-162.94	71.77	-162.82	87.975	59.663	87.92	59.76
713-704	41.576	-56.89	41.52	-56.73	71.81	-162.94	71.77	-162.84	72.346	50.579	72.27	50.67
704-720	25.032	-85.64	24.98	-85.51	52.13	-147.22	52.13	-147.13	67.718	51.755	67.67	51.82
720-707	4.846	-85.72	4.82	-85.53	42.1	-147.21	42.09	-147.18	44.613	38.265	44.59	38.28
707-724	0	0	0	0	9.49	-147.21	9.48	-147.21	9.489	32.793	9.48	32.79
707-722	4.846	-85.72	4.85	-85.71	32.61	-147.21	32.61	-147.22	35.18	39.739	35.18	39.74
720-706	0	0	0.01	0	10.04	-147.25	10.04	-147.2	10.031	32.754	10.03	32.77
706-725	0	0	0	0	10.04	-147.25	10.04	-147.25	10.031	32.754	10.04	32.75
704-714	23.024	-25.38	23.02	-25.33	25.84	163.91	25.82	163.94	4.846	33.91	4.83	34.01
714-718	19.11	-25.37	19.1	-25.37	19.11	154.63	19.1	154.63	0	0	0	0
702-705	21.1	-81.43	21.1	-81.4	20.17	-150.35	20.15	-150.31	34.026	65.008	34.02	65.05
705-742	1.827	-26.72	1.83	-26.71	20.17	-150.35	20.15	-150.35	19.212	34.193	19.2	34.18
705-712	20.1	-85.68	20.11	-85.68	0	0	0	0	20.1	94.324	20.11	94.32
702-703	192.7	-56.21	192.65	-56.13	136.35	167.86	136.21	167.95	134.03	78.763	134.04	78.88
703-727	43.555	-50.59	43.57	-50.56	36.04	167.1	36.03	167.13	26.67	73.738	26.68	73.79
727-744	35.969	-40.91	35.98	-40.89	36.04	167.1	36.04	167.12	17.423	62.89	17.43	62.93
744-729	9.783	-26.73	9.78	-26.72	9.79	153.28	9.78	153.28	0	0	0	0
744-728	17.421	-57.12	17.43	-57.12	17.43	-177.11	17.43	-177.11	17.423	62.89	17.43	62.89
703-730	149.41	-57.85	149.36	-57.77	100.32	168.13	100.2	168.23	107.49	80.008	107.49	80.13
730-709	133.09	-54	133.07	-53.92	100.32	168.13	100.2	168.22	89.297	77.092	89.31	77.23
709-775	0	0	0	0	0	0	0	0	0	0	0	0
709-731	0	0	0	0	19.09	-145.96	19.08	-145.97	19.089	34.04	19.08	34.03
709-708	133.09	-54	133.08	-53.94	88.12	159.18	88	159.26	76.467	86.904	76.52	87.04
708-732	10.193	-87.51	10.2	-87.52	0	0	0	0	10.193	92.49	10.2	92.48
708-733	124.72	-51.42	124.72	-51.35	88.12	159.18	88.02	159.26	66.33	86.047	66.38	86.18
733-734	107.5	-56.02	107.5	-55.96	68.62	160.45	68.54	160.53	66.33	86.047	66.38	86.16
734-710	20.535	-86.27	20.52	-86.21	9.5	-147.34	9.49	-147.07	26.463	75.442	26.47	75.55
710-736	0	0	0	0	9.5	-147.34	9.48	-147.35	9.491	32.662	9.48	32.65
710-735	20.535	-86.27	20.56	-86.28	0	0	0	0	20.535	93.736	20.56	93.72
734-737	82.55	-45.04	82.57	-45	63.25	153.64	63.24	153.68	30.371	93.134	30.4	93.22
737-738	52.65	-56.37	52.67	-56.33	30.65	153.84	30.64	153.89	30.371	93.134	30.4	93.19
738-711	30.371	-86.87	30.38	-86.86	0	0	0.02	0	30.371	93.134	30.4	93.16
711-740	20.59	-86.43	20.61	-86.44	0	0	0	0	20.59	93.575	20.61	93.56
711-741	9.783	-87.8	9.78	-87.81	0	0	0	0	9.783	92.206	9.78	92.19

5.6.3 SPS Analysis

Table 5.11 shows the voltages in per unit and currents in amperes of an 18-node model of the Healy SPS. Node 1 is the slack node; nodes 2-4 are modeled as PV nodes. Table 5.12 shows the generation values. These results have been obtained with 0.001 pu tolerance for power flow as well as PV node convergence. The cables are short, and even a very small voltage difference leads to a large reactive current injection.

Table 5.11: SPS Voltages and Currents

Node ID	|Vab|	∠Vab	From Node-To Node	|Ia|	∠Ia
1	1.02	0	5 - 2	547.55	134.42
2	1.02	0	6 - 3	530.81	137.39
3	1.02	0	6 - 4	530.17	138.61
4	1.02	0	1 - 5	507.68	-41.122
5	1.02	0.007	5 - 6	15.272	-148.53
6	1.02	0.008	5 - 7	507.3	-41.738
7	1.02	-0.002	7 - 8	507.3	-41.738
8	0.987	-10.523	8 - 9	507.3	-41.738
9	0.987	-10.536	5 - 10	510.41	-41.498
10	1.02	0.001	10 - 11	510.41	-41.498
11	0.987	-10.589	11 - 12	510.41	-41.498
12	0.987	-10.603	6 - 13	503.43	-41.573
13	1.02	-0.005	13 - 14	503.43	-41.573
14	0.987	-10.447	14 - 15	503.43	-41.573
15	0.987	-10.464	6 - 16	516.12	-42.101
16	1.02	-0.002	16 - 17	516.12	-42.101
17	0.985	-10.705	17 - 18	516.12	-42.101
18	0.985	-10.721	-	-	-

Table 5.12: SPS Generation

Node ID	Type of Node	Real Power (MW)	Reactive Power (MVAR)
1	Slack	5.808	1.2505
2	PV	6.15	1.5474
3	PV	6.04	1.4476
4	PV	6.06	1.1846

5.7 System Studies on IEEE 37-Node System

The IEEE 37-node feeder without the regulator was studied under different DG modeling and varying penetration.

1. DG is connected to node 734
2. DG penetration is defined as

$$\%DG_{penetration} = \frac{P_{DG}}{P_{total}} * 100 \text{ where, } P_{total} = P_{DG} + P_{sub}$$

3. Anticipating the future load growth, DG penetration is increased by increasing the real and reactive power of loads in all the phases of nodes 727, 728, 729, 730, 731, 732, 733, 735, 736, 737, 738, 740, 741, 742 and 744. The penetration of DG is increased in steps of 3.5% up to 35%, which corresponds to an increase of loading in steps of 5% from 5% to 50% respectively.
4. Figures 5.9-5.11 show a comparison of the voltage deviation from 1 pu for different DG models and varying DG penetration. The x-axis of Figures 5.9-5.11 represents the node number, the y-axis of Figures 5.9 and 5.10 represents the percentage DG penetration and that of Figure 5.11 represents the percentage load increase, and the z-axis of Figures 5.9-5.11 represents the voltage deviation from 1 pu. Figure 5.9 is obtained with DG modeled as a constant PQ node. The surface plot of Figure 5.9 clearly indicates the voltage deviation is low for the downstream nodes of the feeder. The voltage deviation is high for nodes 744 and 728 because the load at node 728 is a three-phase load and, hence, the loading is increased in all three phases, and 744 is directly connected to this node. The minimum voltage deviation is 0.01933 pu. Figure

5.10 is obtained with DG modeled as PV node, which switches to PQ node in case of a reactive power limit hit. The same observations can be made for the surface plot of Figure 5.10. The minimum voltage deviation is 0.0169 pu. Comparing surfaces of Figures 5.9 and 5.10 shows that the difference in voltage deviation for downstream nodes during low DG penetration is not very much. However, the difference in voltage deviation for downstream nodes during high DG penetration is considerable. Figure 5.11 is obtained with the DG modeled as a PV node and a constant penetration of 50%, which switches to a PQ node in case of a reactive power limit hit. However, no reactive power limit hit occurred for the load increases shown.

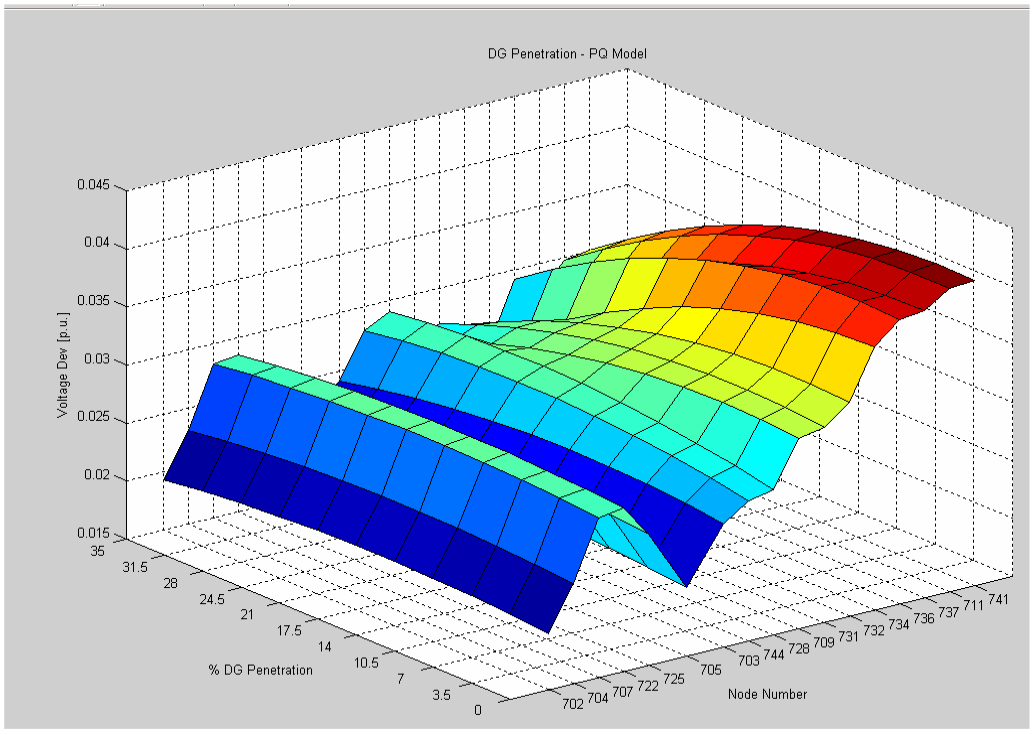

Figure 5.9: IEEE 37-Node Feeder with PQ Model and Varying DG Penetration Level

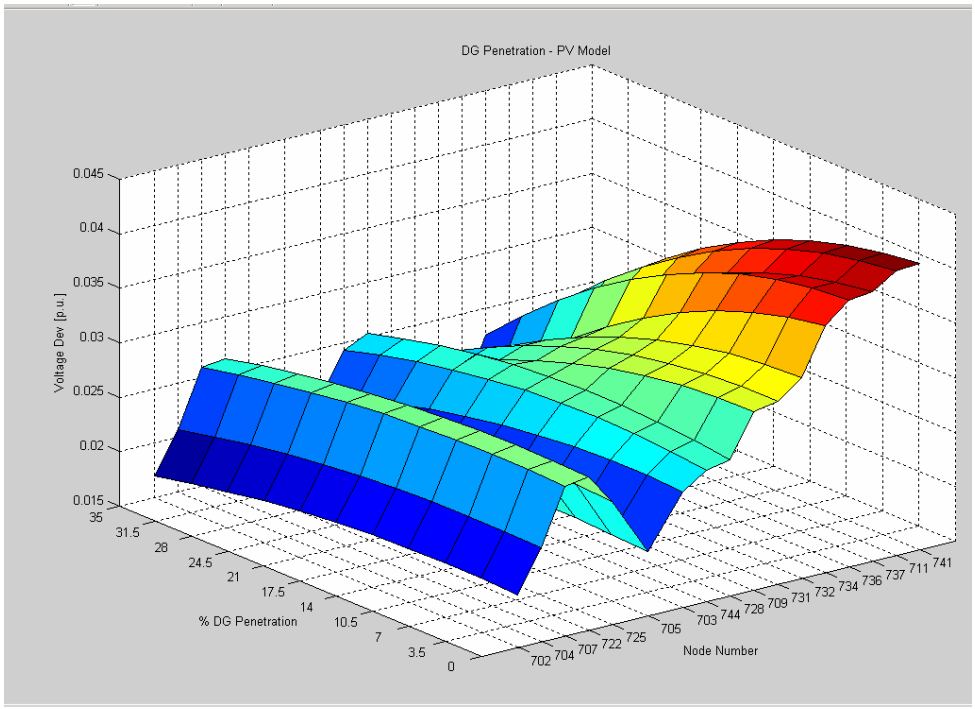

Figure 5.10: IEEE 37-Node Feeder with PV Model and Varying DG Penetration Level

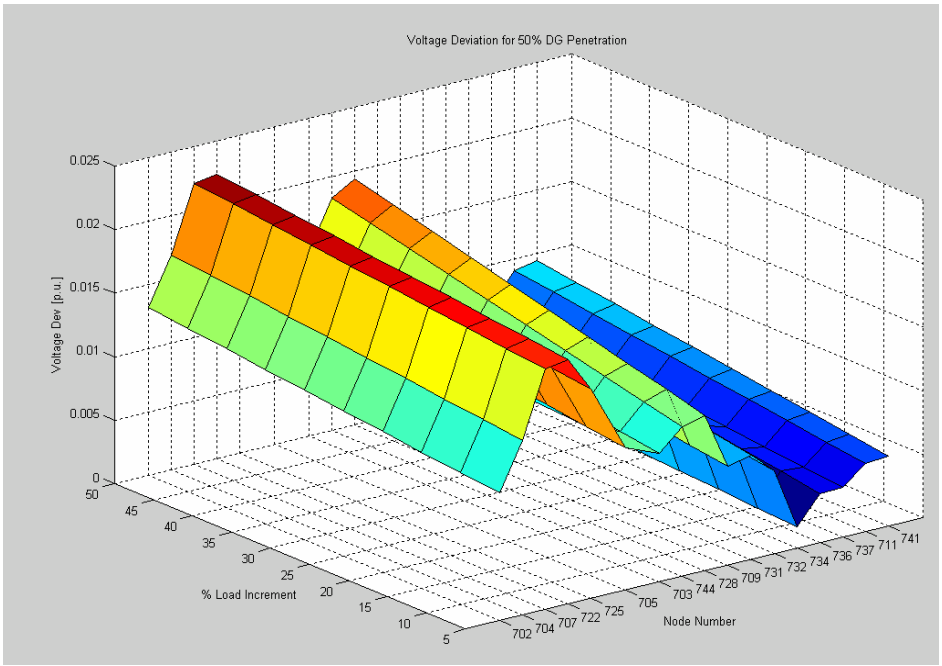

Figure 5.11: IEEE 37-Node Feeder with PV Model and 50% DG Penetration Level

The surface plot of Figure 5.11 clearly indicates the voltage deviation is low for the downstream nodes of the feeder, but it increases with an increase in loading. The minimum voltage deviation is 0.0016 pu. Based on these observations, for an increase in load, the voltage deviation is least when DG is modeled as a PV node with 50% DG penetration.

5. Twelve cases shown in Table 5.13 are defined:

   i) Cases 1-3 are with 0% DG penetration.

   ii) Cases 4-6 are with varying DG penetration but modeled as PQ node.

   iii) Cases 7-9 are with varying DG penetration but modeled as PV node, which switch to PQ node in case of a limit hit.

   iv) Cases 10-12 are with 50% DG penetration but modeled as a PV node, which switches to a PQ node in case of a limit hit. However, for all three cases the limit does not hit with this penetration level.

Table 5.13: Case Scenarios

Case	%DG Penetration	% Increase in load	Model
1	0	5	-
2	0	25	-
3	0	50	-
4	3.5	5	PQ
5	17.5	25	PQ
6	35	50	PQ
7	3.5	5	PV
8	17.5	25	PV
9	35	50	PV
10	50	5	PV
11	50	25	PV
12	50	50	PV

6. Figure 5.12 shows the system loss comparison for all these cases. Losses for cases 1-3, which correspond to no DG penetration, are quite high. Losses for cases 4-6 which correspond to the PQ model, are slightly higher than cases 7-9, which correspond to PV model. For 50% DG penetration, the losses are tremendously decreased. Losses for case 12 are more than that of cases 10 and 11, due to an increase in loading. For a 50% increase in load, losses decrease by 3.4% due to 50% DG penetration.

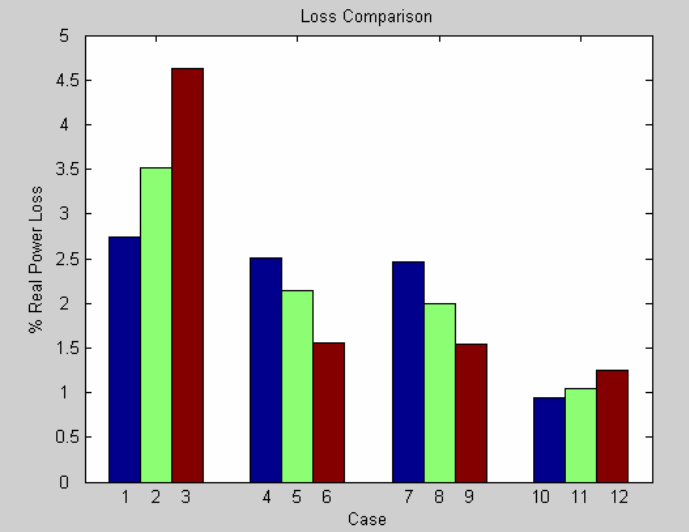

Figure 5.12: IEEE 37-Node Feeder Loss Comparison

7. Figure 5.13 shows the real power generated by the DG relative to that from the substation in all the twelve cases. This graph is also a representation of the DG injection. As seen from the graph for cases 0-3 there is no DG penetration, and hence, the entire real power contribution is from the substation. For cases 4-6 and 7-9, the DG penetration increases and, hence, the substation contribution decreases. For cases 10-12, the DG penetration is 50% and thus, 50% contribution is from the substation.

5.8 Computational Complexity

There was a lot of data due to the three-phase unbalanced nature of the systems. Table 5.14 shows the data required as input for the various components of the system.

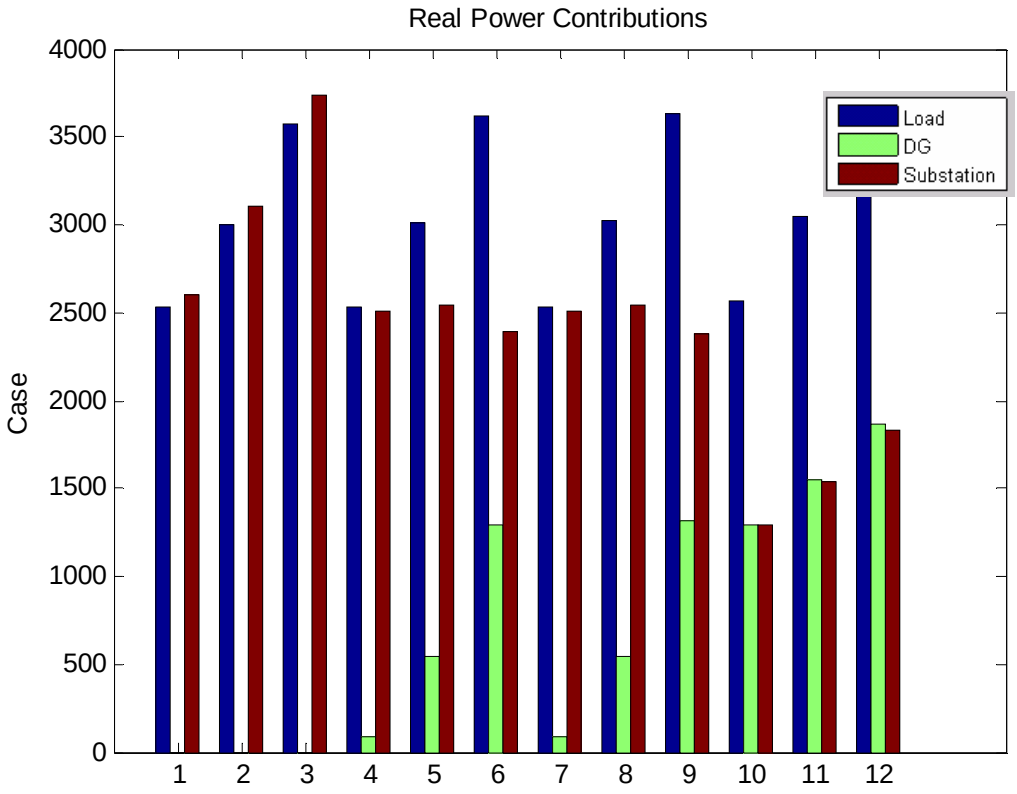

Figure 5.13: Real Power Contributions from DG and Substation along with Total Real Power Loading

The description of the data required is as shown in Table 5.15. The end nodes and junction nodes along with the particular sequence in which the backward trace proceeds, presented a coding challenge. Three-dimensional data structures were utilized for storing the currents according to the sequence of nodes visited. The forward sequence should proceed in exactly the reverse order that the backward sweep proceeds. If a junction node is visited several times, the most recent voltage or current is used for update equations.

The calculation of component currents for delta and wye is different. A DG loop converges outside the power flow loop, and hence initially some convergence issues occured. These issues were solved by clearing some of the variables that needed to be redefined with the DG injection. Multiple DGs require the total reactive current injection of all the DGs, in order to enforce the limits, and this current injection must be calculated at the current power flow solution.

Table 5.14: Data Required for Components

Component	Data Required									
Load	Serial Number	On Node	kW (Ph.A)	kVar (Ph.A)	kW (Ph.B)	kVar (Ph.B)	kW (Ph.C)	kVar (Ph.C)	Connection	Type
Transformer	Primary Connection	Secondary Connection	kVA Rating	VLL High	VLL Low	R (pu)	X (pu)	From Node	To Node	
Line	From Node	To Node	Length	Topology	Config					
Source	On Node	kW (Ph.A)	kVar (Ph.A)	kW (Ph.B)	kVar (Ph.B)	kW (Ph.C)	kVar (Ph.C)	Connection	Type	
Config	ID	Configuration								

Table 5.15: Data Description

Component	Description of Data
Line	Topology- Line Segment is a Transformer - Line Segment is a Regulator Config- Configuration ID
Transformer	Primary Connection- Wye or Delta Secondary Connection- Wye or Delta
Load	Connection- Wye or Delta Type- Constant Current - Constant Power - Constant Impedance
Config	Configuration- 3×3 matrix of impedance

5.9 Summary

This chapter develops component model equations for unbalanced distribution systems. It also describes the backward forward technique. This power flow software, developed in MATLAB, is tested on an IEEE 13-node system and an IEEE 37-node system. RDAP verified the results. The results for the PV model cannot be verified by RDAP, as it does not have that facility. Also, system studies by increased load and DG penetration with different DG models are achieved. The system studies show how DG impacts losses and voltage deviations. These studies also indicate that the developed unbalanced distribution power flow with DG is correct.

CHAPTER VI

CONCLUSIONS AND FUTURE WORK

One of the major aspects of distribution automation is remote control of switching equipment in an optimized and efficient manner in order to obtain an intelligent distribution network. There is growing interest in voltage control, optimized power flow, fault location, restoration, and power quality monitoring which would lead to reliability, customer satisfaction, energy efficiency and environmental benefits. The objectives of an optimized strategy for restoration and efficient and fast unbalanced power flow with multiple sources were achieved by extending existing work as well as developing new algorithms, models and formulation.

6.1 Contributions

Proposed in this dissertation is an optimal method for restoring power after a fault to critical loads, including islanding if necessary. The service restoration problem is formulated for three-phase unbalanced distribution systems. The equations are non-linear with integer variables, making it a difficult problem to solve. Global optimal solutions were obtained for several fault cases. For the IEEE 13-node and 37-node systems, comparisons were made between WSPS and WOSPS schemes, and it was shown that there are trade offs. For the IEEE 37-node system, the search space varies with the fault location.

The formulation does not require separate power flow calculations and gives a complete solution of three phase voltages and currents with the best switching configuration with minimum switch operations. The service restoration problem is also formulated for SPS with IPS and with DG. The optimization involves non-linear equations, which are not linearized, thus removing the linearization assumptions. Out of the several cases studied, one of the cases demonstrates the ability of the restoration method to configure a system within constraints even when islanding.

Also developed in this dissertation is an improved generalized three-phase unbalanced power flow algorithm. This algorithm implemented in a program, can handle multiple source nodes. The IEEE 13-node and IEEE 37-node feeder analyses were performed, and their results were compared with RDAP. DG was introduced at one of the junction nodes for the IEEE 13-node system. This DG node was represented as a PQ node and the results obtained were verified using RDAP. This DG node was then represented as a PV node in the power flow program. RDAP is limited in its capability to model DG as a PV node. The developed software program can also find the steady state solution for SPS. SPS is an ungrounded delta connected system where generation, transmission and distribution are tightly coupled. Analysis of SPS, due to its distinctive characteristics, leads to a further complication in distribution power flow, due to almost the same nominal voltages of all generator nodes. This program can handle multiple DGs and allows for switching the DG mode from constant voltage to constant power factor. System studies showing the impact of considerable DG penetration on the steady state behavior of the California distribution feeder are given. PQ and PV representations along

with different penetration levels are incorporated in the case studies. While finding the power flow solution of a Healy icebreaker ship system, multiple sources are represented as DGs in the software.

6.2 Future Work

As with any research, there is always something more to be done. The first and foremost is enhanced testing and improvement of the developed software. The software can be encoded in languages like C and C++ that can be converted to executable files. Although the optimization is very powerful and avoids a three-phase unbalanced power flow calculation it needs some changes in formulation to make it faster. LINGO is in the process of upgrading its software, which will improve the computational capability of LINGO. SPS are also inherently unbalanced. Further work would involve testing of the restoration formulation for unbalanced terrestrial systems on unbalanced SPS as shown in Figure 6.1. Also optimization can be compared with other decentralized techniques for restoration like Multi Agent Systems (MAS). MAS are fast, but may not give an optimal solution. Thus there is a trade off in optimality and speed between MAS and optimization. By combining these two approaches a reconfiguration system can find a feasible restoration solution quickly and then modify after time towards an optimal solution minimizing the downfalls of each technique individually.

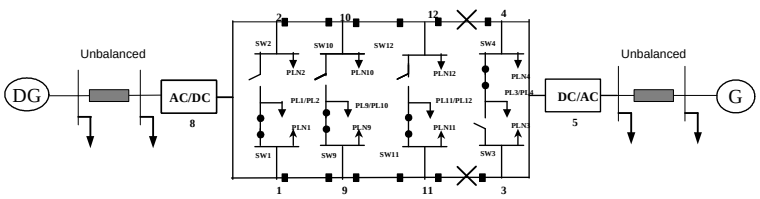

Figure 6.1 Unbalanced Shipboard Power System

It is recommended that the unbalanced power flow software be extended to include DC systems, so as to obtain the steady state solution for SPS having AC and DC components. The software can be a key to the study of DG placement/size under a deregulated environment.

REFERENCES

[1] "White Paper on Distributed Generation," NRECA http://www.nreca.org/nreca/Policy/Regulatory/Documents/DGWhitepaper.pdf

[2] Lindenberg Steve, "Distributed Generation," http://www.nreca.org/edu_events/conferences/newtech/html/track_dg.html

[3] Interconnecting Distributed Resources with Electric Power Systems, IEEE Standard 1547, 2003.

[4] Recommended Practices and Requirements for harmonic Control in Electric Power Systems, IEEE Standard 519-1992, Apr.1993.

[5] Kotamarty S., "Impact of Distributed Generation on Distribution Contingency Analysis," Master of Science Thesis, Mississippi State University, May 2006.

[6] IEEE guide for interfacing dispersed storage and generation facilities with electric utility systems, ANSI/IEEE Standard 1001, 1988.

[7] IEEE Standard for Conformance Test Procedures for Equipment Interconnecting Distributed Resources with Electric Power Systems, IEEE Std 1547.1-2005.

[8] Puttgen Hans et al., "Distributed Generation: Semantic Hype or the Dawn of a New Era?," IEEE Power and Energy Magazine, pp.22-29,January 2003.

[9] Morelato A.L. and Monticelli A.J., "Heuristic search approach to distribution system restoration", IEEE Transactions on Power Delivery, Vol. 4, No. 4, Oct. 1989, pp. 2235 – 2241.

[10] Wu J.S., Tomsovic K.L. and Chen C.S., " A heuristic search approach to feeder switching operations for overload, faults, unbalanced flow and maintenance", IEEE Transactions on Power Delivery, Vol. 6, No. 4, Oct. 1991, pp. 1579 - 1586

[11] Shirmohammadi D., "Service restoration in distribution networks via network reconfiguration", IEEE Transactions on Power Delivery, Vol. 7, No. 2, April 1992, pp. 952 – 958.

[12] Butler K.L., Sarma N.D.R. and Ragendra Prasad V., "Network reconfiguration for service restoration in shipboard power distribution systems", IEEE Transactions on Power Systems, Vol. 16, No. 4, Nov. 2001 pp. 653 – 661.

[13] Nagata T. and Sasaki H., "An efficient algorithm for distribution network restoration", IEEE Power Engineering Society Summer Meeting, Vol. 1, July 2001, pp. 54 – 59.

[14] Toune S., Fudo H., Genji T., Fukuyama Y. and Nakanishi Y., "A reactive tabu search for service restoration in electric power distribution systems", Proceedings of the IEEE International Conference on Evolutionary Computation, 4-9 May 1998, pp. 763 – 768.

[15] Hsiao Y. and Chien C., "Enhancement of restoration service in distribution systems using a combination fuzzy-GA method", IEEE Transactions on Power Systems, Volume 15, No. 4, Nov. 2000, pp. 1394 - 1400.

[16] Fukuyama Y., "Reactive Tabu Search for Distribution Load Transfer Operation," Proceedings of IEEE Power Engineering Society Winter Meeting, Vol. 2, pp. 1301-1306, Jan. 2000.

[17] Chao-Shun Chen, Chia-Hung Lin and Hung-Ying Tsai, "A rule-based expert system with colored Petri net models for distribution system service restoration", IEEE Transactions on Power Systems, Vol. 17, No. 4, Nov. 2002, pp. 1073 – 1080.

[18] Butler, K.L., Momoh, J.A. and Dias, L.G., "Expert system assisted identification of line faults on delta-delta distribution systems", Proceedings of the 35th Midwest Symposium on Circuits and Systems, Vol. 2, 9-12 Aug. 1992, pp. 1208 – 1213.

[19] Qin Zhou, Shirmohammadi D. and Liu W., "Distribution feeder reconfiguration for service restoration and load balancing", IEEE Transactions on Power Systems, Vol. 12, No. 2, May 1997, pp. 724 – 729.

[20] Chen C.S., Lin C.H., Wu C.J. and Kang M.S., "Feeder reconfiguration for distribution system contingencies by object oriented programming", IEEE Power Engineering Society Summer Meeting, 2000, Vol. 1, 16-20 July 2000, pp. 431 – 436.

[21] Jiansheng Lei, Youman Deng, Ying He and Boming Zhang, "Network reconfiguration in unbalanced distribution systems for service restoration and loss reduction", IEEE Power Engineering Society Winter Meeting, Vol. 4, 23-27 Jan. 2000, pp. 2345 – 2350.

[22] Jin-Cheng Wang, Hsiao-Dong Chiang and Darling G.R., "An efficient algorithm for real-time network reconfiguration in large scale unbalanced distribution systems" IEEE Transactions on Power Systems, Vol. 11, No. 1, Feb.1996, pp. 511 – 51.

[23] Borozan, V., Rajicic, D. and Ackovski, R., "Minimum loss reconfiguration of unbalanced distribution networks", IEEE Transactions on Power Delivery, Vol. 12, No. 1, Jan. 1997, pp. 435 – 442.

[24] Jinxiang Zhu, Mo-Yuen Chow and Fan Zhang, "Phase balancing using mixed-integer programming", IEEE Transactions on Power Systems, Vol. 13, No. 4, Nov. 1998, pp. 1487 – 1492.

[25] Baran M.E. and Wu F.F., "Network reconfiguration in distribution systems for loss reduction and load balancing", IEEE Transactions on Power Delivery, Vol. 4, No. 2, April 1989, pp. 1401 – 1407.

[26] Luan W.P., Irving, M.R. and Daniel, J.S., "Genetic algorithm for supply restoration and optimal load shedding in power system distribution networks," IEE Proceedings on Generation, Transmission and Distribution, Vol. 149, Issue 2, March 2002, pp. 145 - 151.

[27] Watanabe I. and Nodu M., "A genetic algorithm for optimizing switching sequence of service restoration in distribution systems," Proceedings of the Congress on Evolutionary Computation, Vol. 2, 19-23 June 2004, pp. 1683 - 1690.

[28] Mantawy A.H. and Al-Ghamdi M.S., "A new reactive power optimization algorithm," Proceedings of the IEEE Power Tech Conference, Vol. 4, 23-26 June 2003, pp.6-11, Bologna.

[29] Toune S., Fudo H., Genji T., Fukuyama Y. and Nakanishi Y., "Comparative study of modern heuristic algorithms to service restoration in distribution systems", IEEE Transactions on Power Delivery, Vol. 17, No. 1, Jan. 2002, pp. 173 – 181.

[30] Chiang H.-D. and Jean-Jumeau R., "Optimal network reconfigurations in distribution systems. I. A new formulation and a solution methodology," IEEE Transactions on Power Delivery, Vol. 5, Issue 4, Oct 1990, pp. 1902 – 1909.

[31] Mori H. and Ogita. Y., "A parallel tabu search based method for determining optimal allocation of FACTS in power systems," Proceedings of the International Conference on Power System Technology, Vol. 2, 4-7 Dec 2000, pp. 1077 - 1082.

[32] Lee S.J., Kim K.H., Kim H.Y., Lee J.K. and Nam K.Y., "Expert system-aided service restoration in distribution automation," IEEE International Conference on Systems Man and Cybernetics, Vol. 1, 18-21 Oct 1992, pp. 157 - 161

[33] Liu C.-C., Lee S.J. and Venkata, S.S., "An expert system operational aid for restoration and loss reduction of distribution systems," IEEE Transactions on Power Systems, Vol. 3, Issue 2, May 1988 pp. 619 - 626 .

[34] Butler-Purry K.L., Sarma N.D.R. and Hicks I.V., "Service restoration in naval shipboard power systems," IEE Proceedings on Generation, Transmission and Distribution, Vol. 151, Issue 1, 14 Jan 2004, pp.95 - 102.

[35] Das D., Nagi H.S. and Kothari, D.P., "Novel method for solving radial distribution networks," IEE Proceedings of the Generation, Transmission and Distribution, Vol. 141, Issue 4, July 1994, pp.291 - 298.

[36] Nanda J., Srinivas M.S., Sharma M., Dey S.S. and Lai, L.L., "New findings on radial distribution system load flow algorithms," Proceedings of the IEEE Power Engineering Society Winter Meeting, Vol. 2, 23-27 Jan 2000, pp. 1157 - 1161.

[37] Zimmerman Ray D. and Chiang H.D., "Fast Decoupled Power Flow for Unbalanced Radial Distribution Systems" IEEE Transactions on Power Systems, Vol.10, No.4, Nov. 1995, pp. 2045-2052.

[38] H. K. Mok, S. Elangovan, M. M. A. Salama and Cao Longjian, "Power Flow Analysis for Balanced and Unbalanced Radial Distribution Systems," http://www.itee.uq.edu.au/~aupec/aupec99/mok99.pdf

[39] Chen T. H., Chen M. S., Hwang K. J., Kotas P. and Chebli, E.A., "Distribution system power flow analysis-a rigid approach," IEEE Transactions on Power Delivery, Vol. 6, Issue 3, July 1991, pp. 1146 - 1152.

[40] Teng J. H., "A Network-Topology Based Three-Phase Load Flow for Distribution Systems," Proceedings of National Science Council ROC (A), Vol. 24, no. 4, pp. 259-264, 2000.

[41] Xu W., Dommel H.W. and Marti J.R., "A generalised three-phase power flow method for the initialisation of EMTP simulations," Proceedings of the International Conference on Power System Technology, Vol. 2, 18-21 Aug 1998, pp. 875 - 879.

[42] Lin Whei-Min, Su Yuh-Sheng, Chin Hong-Chan and Teng Jen-Hao, "Three-phase unbalanced distribution power flow solutions with minimum data preparation," IEEE Transactions on Power Systems, Vol. 14, Issue 3, Aug 1999, pp. 1178 - 1183.

[43] Birt K. A., Graffy J. J., McDonald J.D. and El-Abiad A. H., "Three Phase load flow program," IEEE Transactions on Power Apparatus and Systems, Vol. PAS-95, No. 1, Jan/Feb 1976, pp. 59-65.

[44] Nanda J., Kothari M. and Srinivas M.S., "On some aspects of distribution load flow," IEEE Region 10 International Conference on Global Connectivity in Energy, Computer, Communication and Control, Vol. 2, 17-19 Dec 1998, pp. 510 – 513.

[45] Laughton M.A., "Analysis of unbalanced polyphase networks by method of phase co-ordinates," Proceedings of the IEE, Vol. 15, No.8, August 1968.

[46] Jang Y. J. and Park J. K., "Three-Phase Power Flow Method based on Fast-decoupled Method for Unbalanced Radial Distribution System," http://eeserver.korea.ac.kr/~bk21/arch/bk21conf/54.pdf

[47] Srinivas M. S., "Distribution Load Flows: A brief review," Proceedings of IEEE PES Winter Meeting, Jan 2000, Vol. 2, pp.942 – 945.

[48] Luo G.X. and Semlyen A., "Efficient load flow for large weakly meshed networks," IEEE Transactions on Power Systems, Vol. 5, Issue 4, Nov 1990, pp. 1309 - 1316.

[49] Shirmohammadi D., Hong H.W., Semlyen A. and Luo, G.X., "A compensation-based power flow method for weakly meshed distribution and transmission networks," IEEE Transactions on Power Systems, Vol. 3, Issue 2, May 1988, pp. 753 - 762.

[50] Chen T.-H., Chen M.-S., Inoue T., Kotas, P. and Chebli, E.A., "Three-phase cogenerator and transformer models for distribution system analysis," IEEE Transactions on Power Delivery, Vol. 6, Issue 4, Oct 1991, pp. 1671 - 1681.

[51] Abur A., Singh H., Liu H. and Klingensmith W. N., "Three Phase Power Flow for Distribution Systems with Dispersed Generation," http://www.eeh.ee.ethz.ch/pscc02/papers/s11p03.pdf

[52] Cheng Carol S. and Shirmohammadi Dariush, "A Three-Phase Power Flow Method for Real-Time Distribution System Analysis" IEEE Transactions on Power Systems, Vol.10, No.2, May. 1995.

[53] Losi, A. and Russo, M., "Dispersed generation modeling for object-oriented distribution load flow," IEEE Transactions on Power Delivery, Vol. 20, Issue 2, P-2, April 2005, pp. 1532 – 1540

[54] Medina M. M., Qi L. and Butler-Purry K. L., "A Three-Phase Load Flow Algorithm for Shipboard Power Systems (SPS)," Proceedings of the IEEE PES Transmission and Distribution Conference and Exposition, Vol. 1, pp. 227 – 233, Sept 2003.

[55] Baldwin T. L. and Lewis S. A., "Distribution Load Flow Methods for Shipboard Power Systems," IEEE Transactions on Industry Applications, Vol. 40, No. 5, pp. 1183 – 1190, Sept-Oct 2004.

[56] USCGC Healy, http://www.ces.clemson.edu/powsys2002/ppt/P5/TB.ppt

[57] Chester Petry R. and Rumburg Jay W.," Zonal Electrical Distribution Systems: An affordable Architecture for Future", Naval Engineers Journal, May 1993, pp. 45-51.

[58] LINDO Systems Inc., Chicago IL, Release-8, 2003.

[59] RDAP User Manual, Version 3.0, September 1999, WH Power Consultants, Las Cruces, NM. http://www.zianet.com/whpower

[60] Khushalani Sarika and Schulz Noel N., "Optimized Restoration of Shipboard Power Systems with IPS Architecture and Distributed Generation", Proceedings of the ASNE Reconfiguration and Survivability Symposium, Jacksonville, USA, Feb 2005.

[61] Khushalani Sarika, Solanki Jignesh M. and Schulz Noel N., "Optimized Restoration of Unbalanced Distribution Systems", Submitted for review to IEEE Transactions on Power Systems, March 2006.

[62] Zhang Fan and Cheng C.S., "A modified Newton method for radial distribution system power flow analysis," IEEE Transactions on Power Systems, Vol. 12, Issue 1, Feb 1997, pp. 389 - 397

[63] Wang L., Xiang P., Wang S., Zhang B. and Huang M., "Novel decoupled power flow," IEE Proceedings C on Generation, Transmission and Distribution, Vol. 137, Issue 1, Jan 1990, pp.1 – 7.

[64] Billo Jeffrey, "Models and Methods for Shipboard Power System Reconfiguration," Master of Science Thesis, University of Texas at Austin, Dec. 2003.

[65] Radial Distribution Test Feeders, http://www.ewh.ieee.org/soc/pes/dsacom/testfeeders.html

[66] Khushalani Sarika and Schulz Noel N., "Unbalanced Distribution Power Flow with Distributed Generation," Proceedings of the IEEE Transmission and Distribution Conference, Dallas, USA, May 2006.

[67] Khushalani Sarika, Solanki Jignesh M. and Schulz Noel N., "Development of Three Phase Unbalanced Power Flow with Multiple Distributed Generators and study of

their Impact on Distribution Systems," Submitted for review to IEEE Transactions on Power Systems, March 2006.

[68] Kersting, W.H., "Radial distribution test feeders," Proceedings of IEEE PES Winter Meeting, Vol.2, pp. 908 –912, 2001.

[69] Kersting, W.H., Distribution System Modeling and Analysis, CRC Press, New York, 2002.